Phase-ordering kinetics with external fields and biased initial conditions

J. A. N. Filipe,[1,*] A. J. Bray,[1] and Sanjay Puri[2]

[1] *Theoretical Physics Group, Department of Physics and Astronomy, The University, Manchester M13 9PL, United Kingdom*

[2] *School of Physical Sciences, Jawaharlal Nehru University, New Delhi 110067, India*

(Received 24 February 1995)

The late-time phase-ordering kinetics of the $O(n)$ model for a nonconserved order parameter are considered for the case where the $O(n)$ symmetry is broken by the initial conditions or by an external field. An approximate theoretical approach, based on a "Gaussian closure" scheme, is developed, and results are obtained for the time dependence of the mean order parameter, the pair correlation function, the autocorrelation function, and the density of topological defects [e.g., domain walls ($n = 1$), or vortices ($n = 2$)]. The results are in qualitative agreement with experiments on nematic films and related numerical simulations on the two-dimensional XY model with biased initial conditions.

PACS number(s): 64.60.Cn, 64.60.My

I. INTRODUCTION

The field of phase-ordering kinetics has seen a resurgence of interest in recent years [1]. It is by now well established that in the late stages of ordering a scaling regime is entered, characterized by a single time-dependent length scale $L(t)$. The existence of a single characteristic scale has the consequence, for example, that the pair correlation function for the order parameter field exhibits the scaling form $C(\mathbf{r},t) = f(r/L(t))$, where $f(x)$ is a scaling function. Systems with nonscalar order parameters have attracted special attention recently, partly in response to experimental interest in liquid crystal systems [2]. In particular, approximate methods developed for calculating scaling functions for scalar fields [3, 4] have been extended to vector fields [7, 5, 6]. So far, however, little effort has been devoted to the role of external fields, or a symmetry-breaking bias in the initial conditions. For systems with nonconserved order parameter, with which this paper is exclusively concerned, these effects are important because in the experimental context it may be difficult to ensure the conditions of perfect symmetry (i.e., the absence of any symmetry breaking in the dynamics or in the initial conditions) required for the "critical quenches" usually studied by theorists. Recent work on nematic liquid crystal films [8] provides a concrete example which we will discuss in detail.

In this paper we study the phase-ordering dynamics of systems with nonconserved order parameter, in situations where an external field is present and/or the initial state contains a bias. We may call these systems "off critical," as opposed to critical systems whose initial state and dynamics are rotationally invariant (or inversion symmetric for scalar fields). An immediate difference relative to critical quenches is that the system will (in most cases) reach global saturation exponentially fast, thus limiting the duration of the scaling regime. We study both scalar and vector systems. In the former there is a simple magnitude relaxation of the order parameter, while in the latter there is also a slower orientational process. Physical realizations are spin systems (magnets), nematic liquid crystals, and order-disorder transitions in binary alloys. The problem is addressed using an analytically solvable approach, the *systematic approach* (SA) [9], which is a form of "Gaussian closure" approximation. At leading order, it reproduces the results of earlier approximation schemes [3,7], but has the virtue that it is (at least in principle) systematically improvable [10]. We derive an approximate linear equation for an auxiliary field $\tilde{m}$. This equation is exact in the limits $n \to \infty$ or $d \to \infty$, where n and d are the spin and space dimensions, respectively. From this we obtain predictions for the mean order parameter, the topological defect density, and the pair correlation function.

The systematic approach was developed by Bray and Humayun (BH) [9] for simple nonconserved dynamics with no field or bias, in which case the results of Ohta, Jasnow, and Kawasaki (OJK) [3] and the extension thereof to vector fields by Bray and Puri and Toyoki (BPT) [7] are recovered in leading order. This approach has the virtue, however, that it can in principle be systematically improved. We are not concerned here with the possibility of improving the leading order calculations, which is a problem of great technical difficulty [11], but in showing that the approach (in lowest order) can be successfully extended to off-critical systems.

In Sec. II we discuss the original systematic approach. For simplicity we begin with scalar fields. The extension to vector fields is straightforward. In Sec. III we generalize the scheme to include a time-dependent external field and an initial bias. In this case the relevant phenomenon is different for scalar and vector systems and so the con-

*Present address: Physics Department, Brunel University, Uxbridge UB8 3PH, United Kingdom.

struction of the approach is also different. For scalars the important effect of the field is a domain-wall driving force, while for vectors the bulk rotation of the order parameter plays an important role. The magnetization is compared with an earlier prediction from the large-n solution of the time-dependent Ginzburg-Landau (TDGL) equation, by Bray and Kissner (BK) [12]. We also compare the predictions for the planar XY model with an initial bias with data from experiment and simulations on nematic liquid crystals [8].

II. CRITICAL QUENCHES

An appropriate free-energy functional to describe a phase-ordering system is the Ginzburg-Landau form

$$F[\vec{\phi}] = \int d^d x \left[\frac{1}{2} \left(\vec{\nabla} \vec{\phi} \right)^2 + V(\vec{\phi}) \right] , \tag{1}$$

where $V(\vec{\phi})$ is a sombrero potential, e.g., $V(\vec{\phi}) = (1 - \vec{\phi}^2)^2$, with a degenerate ground state manifold $\vec{\phi}^2 = 1$. For scalar systems, the potential has the usual double-well structure, and the ground state has a discrete, twofold degeneracy.

An appropriate equation of motion for nonconserved dynamics is given by the TDGL equation

$$\frac{\partial \vec{\phi}}{\partial t} = -\frac{\delta F}{\delta \vec{\phi}} = \nabla^2 \vec{\phi} - \frac{dV}{d\vec{\phi}} . \tag{2}$$

We will consider scalar and vector systems in turn.

A. Scalar fields

According to the seminal work of Allen and Cahn [13], the motion of the interfaces in nonconserved systems is determined, in the absence of a bulk driving force, solely by their local curvature. The detailed form of the potential $V(\phi)$ and the particular distribution of initial conditions are not important to the late-stage dynamics, and therefore to the scaling properties. The only relevant feature of $V(\phi)$ is the double-well structure, which generates and maintains well-defined interfaces, while its detailed shape only affects the short-distance behavior, such as the domain-wall profile. Similarly, the details of the initial random configuration determine the early-stage locations of the walls which, in the absence of any systematic bias, should be irrelevant to the scaling properties. The systematic approach exploits this freedom through a convenient choice of $V(\phi)$ and initial conditions.

The TDGL equation (2) for the evolution of a nonconserved, scalar field $\phi(\mathbf{r}, t)$ reads (where primes indicate derivatives)

$$\frac{\partial \phi}{\partial t} = \nabla^2 \phi - V'(\phi) . \tag{3}$$

In the "Gaussian closure" schemes [9, 3, 7, 14, 6, 5] a new field $m(\mathbf{r}, t)$ is introduced, which varies smoothly on the domain scale and whose zeros define the positions of the walls. Following Mazenko [14], the transformation $\phi(m)$ is defined by the equilibrium planar profile of an isolated wall, which satisfies

$$\phi''(m) = V'(\phi) , \tag{4}$$

with boundary conditions

$$\phi(\pm\infty) = \pm 1 \quad , \quad \phi(0) = 0 . \tag{5}$$

With this choice, near a wall (where this can be regarded as flat) m plays the role of a distance from the wall, while inside the domains m is typically of order $L(t)$. Rewriting Eq. (3) in terms of m, and using (4) to eliminate V', gives

$$\dot{m} = \nabla^2 m - \frac{\phi''(m)}{\phi'(m)} \left[1 - (\vec{\nabla} m)^2 \right] . \tag{6}$$

The nonlinear profile function $\phi(m)$ depends on the potential $V(\phi)$, so for general potentials Eq. (6) offers no obvious simplification over the original TDGL equation (3). As argued above, however, the scaling functions should be insensitive to the potential, and thus to the details of the profile function. The results of the OJK [3] and Mazenko [14] approaches, for instance, make no explicit reference to the potential. The key step in the present approach is to exploit this idea, by choosing a particular form of $V(\phi)$ such that Eq. (6) is simplified.

Bray and Humayun (BH) [9] chose the profile function to satisfy

$$\phi''(m) = -m\, \phi'(m) , \tag{7}$$

which is equivalent, via (4), to a particular form of the potential, as shown below. Integrating (7) with the boundary conditions (5) gives the wall profile function

$$\begin{aligned} \phi(m) &= \sqrt{2/\pi} \int_0^m dx \, \exp\left(-x^2/2\right) \\ &= \mathrm{erf}\left(m/\sqrt{2} \right) , \end{aligned} \tag{8}$$

where $\mathrm{erf}(x)$ is the error function. On the other hand, integrating (4) once, with the zero of the potential defined by $V(\pm 1) = 0$, gives

$$V(\phi) = (1/2)\, (\phi')^2 \; = \; (1/\pi)\, \exp(-m^2) \tag{9}$$

$$= (1/\pi)\, \exp\left(-2 \left\{ \mathrm{erf}^{-1}(\phi) \right\}^2 \right) , \tag{10}$$

where $\mathrm{erf}^{-1}(x)$ is the inverse error function. Note that (8) is a monotonic mapping, with the constraint $\phi^2 \leq 1$ due to the boundary conditions (5). It follows that (10) only determines $V(\phi)$ within the region $\phi^2 \leq 1$. For instance, we have $V(\phi) \simeq 1/\pi - \phi^2/2$ for $\phi^2 \ll 1$, while $V(\phi) \simeq (1/4)(1 - \phi^2)^2 \, |\ln(1 - \phi^2)|$ for $\phi^2 \simeq 1$. At a temperature of $T = 0$, however, if the initial condition satisfies $\phi^2(\mathbf{r}, 0) \leq 1$ everywhere, the equation of motion (3) implies that $\phi^2(\mathbf{r}, t) \leq 1$ everywhere at any later time. So $\phi(\mathbf{r}, t)$ does not depend on $V(\phi)$ for $\phi^2 > 1$, and there is no need to know the potential in this region [if $T > 0$, however, the points $\phi = \pm 1$ must be global minima of $V(\phi)$, in order to ensure stability against thermal fluctuations].

With the choice (7), Eq. (6) reduces to

$$\dot{m} = \nabla^2 m + \left[1 - (\vec{\nabla} m)^2\right] m \ . \tag{11}$$

This equation, though still nonlinear, is much simpler than the original TDGL equation, while retaining the physical ingredients essential to describe the universal scaling properties. To make further progress, and to recover the usual OJK results, one simply replaces $\left(\vec{\nabla} m\right)^2$ by its average (over the initial conditions)

$$\left(\vec{\nabla} m\right)^2 \to \left\langle \left(\vec{\nabla} m\right)^2 \right\rangle \ . \tag{12}$$

Then (11) becomes the self-consistent linear equation for $m(\mathbf{r}, t)$:

$$\dot{m} = \nabla^2 m + a(t)\, m \ , \tag{13}$$

with

$$a(t) = 1 - \left\langle (\nabla m)^2 \right\rangle \ . \tag{14}$$

As in OJK's theory, to proceed with the calculations one takes the initial conditions for m to be Gaussian distributed, with zero mean and correlator (in Fourier space)

$$\langle m_{\mathbf{k}}(0) m_{\mathbf{k}'}(0) \rangle = \Delta (2\pi)^d \delta(\mathbf{k} + \mathbf{k}') \ , \tag{15}$$

representing short-range spatial correlations at $t = 0$. Hence, from (13), $m(\mathbf{r}, t)$ is a Gaussian field at all times. The formal solution of (13) in Fourier space is

$$m_{\mathbf{k}}(t) = m_{\mathbf{k}}(0) \exp\left[-k^2 t + b(t)\right] \ , \tag{16}$$

with the definition

$$b(t) = \int_0^t dt'\, a(t') \ . \tag{17}$$

The function $b(t)$ is determined self-consistently, as follows. Inserting (16) and (17) into definition (14) gives

$$a(t) = db/dt$$

$$= 1 - \Delta \exp[2b(t)] \int \frac{d^d k}{(2\pi)^d} k^2 \exp\left(-2k^2 t\right) \ . \tag{18}$$

Although this equation can be readily solved for the whole time range after the quench, it suffices for our purposes to extract the large-t behavior of $b(t)$ which is most easily obtained directly from (18). In the scaling limit we expect that $a(t) \to 0$ [in fact we expect that $a(t) \sim 1/t$ if all terms in (13) scale the same way]. Neglecting the left-hand side of (18) and performing the momentum integral gives

$$\exp[b(t)] \simeq (t/t_0)^{\frac{d+2}{4}} \ , \quad t \gg t_0 \ , \tag{19}$$

with the definition

$$t_0^{\frac{d+2}{2}} = \frac{d\Delta}{4(8\pi)^{d/2}} \ . \tag{20}$$

From (19) we immediately get

$$a(t) \simeq \frac{d+2}{4t} \ , \quad t \gg t_0 \ , \tag{21}$$

confirming the consistency of the previous assumption. The short-time cutoff t_0 was introduced as a device to prevent the breakdown of the momentum integral in (18) as $t \to 0$. It is equivalent to imposing a large-k cutoff (of order $1/t_0^{1/2}$) associated with the smallest length in the system (e.g., the defect core size ζ), which removes the mathematical singularities. So t_0 should be small. The condition $t \gg t_0$ characterizes the times for which the above asymptotic forms are valid, i.e., it defines the scaling regime [$L(t) \gg \zeta$] in which we are interested. Throughout this paper we will, however, for computational convenience, take t down to t_0 while still using (19). This implies that the calculated scaling functions will neither be accurate nor universal in the early-time regime $t \sim t_0$, but will not affect their behavior in the true scaling regime. In this regime, the scaling functions will not depend on the specific way in which the cutoff has been introduced.

Having determined $b(t)$, we may use (19) to write the explicit result for $m_{\mathbf{k}}(t)$, valid for large t,

$$m_{\mathbf{k}}(t) = m_{\mathbf{k}}(0)\ (t/t_0)^{\frac{d+2}{4}} \exp(-k^2 t) \ , \tag{22}$$

from which the two-time correlator, in Fourier and real space, follows immediately:

$$\langle m_{\mathbf{k}}(t_1) m_{-\mathbf{k}}(t_2) \rangle = \Delta \left(t_1 t_2 / t_0^2\right)^{\frac{d+2}{2}} \exp\left[-k^2 (t_1 + t_2)\right] \ , \tag{23}$$

and

$$C_0(1,2) \equiv \langle m(1) m(2) \rangle = \frac{4\sqrt{t_1 t_2}}{d} \left(\frac{4 t_1 t_2}{(t_1 + t_2)^2}\right)^{d/4} \times \exp\left(-\frac{r^2}{4(t_1 + t_2)}\right) \ , \tag{24}$$

where 1 and 2 are the usual shorthand for space-time points $(\mathbf{r}_1, t_1)$ and $(\mathbf{r}_2, t_2)$, and $r = |\mathbf{r}_1 - \mathbf{r}_2|$. From this, we find the expected scaling form

$$S_0(t) \equiv \left\langle m^2 \right\rangle = \frac{4t}{d} \sim L(t)^2 \ , \tag{25}$$

in agreement with the physical interpretation of m as a length. It is interesting that the linear term $a(t)m$ in (13), with $a(t)$ given by (21), exactly reproduces the Oono-Puri extension of the OJK theory [15], designed to eliminate the implicit time dependence of the interface width, which is unphysical. The resulting difference in the time factors of (24) and (25), however, does not affect the scaling functions, which as usual only depend on the normalized correlator

$$\gamma(1,2) \equiv \frac{\langle m(1) m(2) \rangle}{\sqrt{\langle m(1)^2 \rangle \langle m(2)^2 \rangle}} = \left(\frac{4 t_1 t_2}{(t_1 + t_2)^2}\right)^{d/4} \exp\left(-\frac{r^2}{4(t_1 + t_2)}\right) \ . \tag{26}$$

Finally, we evaluate the correlation function of the field ϕ. Since from (25) m is typically of order $\sqrt{t}$ at late times, it follows from (8) that the field ϕ saturates ($\phi = \pm 1$) almost everywhere at late times. As a consequence, we can make the usual simplification $\phi(m) = \mathrm{sgn}(m)$ as far as scaling properties are concerned. The calculation of the average $C(1,2) = \langle \mathrm{sgn}[m(1)]\mathrm{sgn}[m(2)] \rangle$ for a Gaussian field $m(\mathbf{r},t)$ is the same as in the OJK theory (see the Appendix). Therefore the OJK scaling function $C(12) = (2/\pi)\sin^{-1}[\gamma(1,2)]$ is recovered.

We conclude this subsection with a technical remark on the above procedure. To make the replacement (12) in a controlled way, BH systematize the treatment by attaching to the field m an internal "color" index α, running from 1 to N, and generalizing (11) to

$$\dot{m}_\alpha = \nabla^2 m_\alpha + \left(1 - (1/N)\sum_{\beta=1}^{N} (\nabla m_\beta)^2\right) m_\alpha \ . \tag{27}$$

Equation (11) is the case $N = 1$. In the limit $N \to \infty$ the "color" sum is replaced by its average, giving the linear equation (13) (with m standing for one of the m_α). This procedure allows, in principle, for a systematic treatment of the results in powers of $1/N$. The replacement (12) is also justified in the limit $d \to \infty$, when $(\nabla m)^2$ is also a sum of a large number of random variables with relative fluctuations $\sim 1/\sqrt{d}$. This scheme, though less simple to systematize [9], makes clear that the leading order results become exact for large d. We stress, however, that we are not concerned here with the calculation of $O(1/N)$ corrections to the previous results. Our purpose is to extend the leading order calculations to off-critical systems.

B. Vector fields

For nonconserved vector fields, the starting point is the TDGL equation in the form (2). This time a *vector* field $\vec{m}(\mathbf{r},t)$ is introduced, whose zeros define the locations of the topological defect cores. The transformation $\vec{\phi}(\vec{m})$ is now defined by an equilibrium solution of (2), which satisfies the vector analogue of (4) [6, 5]

$$\nabla_m^2 \vec{\phi} = dV/d\vec{\phi} \ , \tag{28}$$

where $\nabla_m^2 = \sum_{\alpha=1}^{n} \partial^2/\partial m_\alpha^2$ is the Laplacian in $\vec{m}$ space. We look for a radially symmetric solution of (28):

$$\vec{\phi}(\vec{m}) = g(\rho)\,\hat{\vec{m}} \ , \tag{29}$$

where $\rho \equiv |\vec{m}|$ and $\hat{\vec{m}} \equiv \vec{m}/|\vec{m}|$, with boundary conditions

$$g(\infty) = 1 \quad , \quad g(0) = 0 \ , \tag{30}$$

[though any solution differing from (29) by a global rotation is equally acceptable]. Thus $g(\rho)$ is the equilibrium profile function for a topological defect in the field $\vec{\phi}$, with $|\vec{m}|$ representing the distance from the defect core [6, 5].

A solution of this form makes sense, of course, only for $n \le d$ when singular topological defects exist. Rewriting the TDGL equation (2) for each component of $\vec{\phi}$ in terms of $\vec{m}$, and using (28) to eliminate $dV/d\phi_a$, gives

$$\sum_b \frac{\partial \phi_a}{\partial m_b}\frac{\partial m_b}{\partial t} = \sum_b \frac{\partial \phi_a}{\partial m_b}\nabla^2 m_b + \sum_{bc} \frac{\partial^2 \phi_a}{\partial m_b \partial m_c}\vec{\nabla} m_b \cdot \vec{\nabla} m_c - \nabla_m^2 \phi_a \ . \tag{31}$$

As in the scalar case, in order to establish a linear equation for $\vec{m}$ one replaces the quadratic factor $\vec{\nabla} m_b \cdot \vec{\nabla} m_c$ by its average (over the initial conditions):

$$\vec{\nabla} m_b \cdot \vec{\nabla} m_c \to \left\langle \left(\vec{\nabla} m\right)^2 \right\rangle \delta_{bc} \ . \tag{32}$$

Here we used the fact that $\left\langle (\vec{\nabla} m_b)^2 \right\rangle$ is independent of b, from global isotropy, to write it as $\left\langle (\vec{\nabla} m)^2 \right\rangle$ where m is any component of $\vec{m}$. As before, one can attach an additional "color" index α ($= 1, \ldots, N$) to the vector $\vec{m}$, such that the replacement (32) corresponds to taking the limit $N \to \infty$ in the theory. In this case, however, it also corresponds to the limit $n \to \infty$. With (32), (31) simplifies to

$$\sum_b \frac{\partial \phi_a}{\partial m_b}\frac{\partial m_b}{\partial t} = \sum_b \frac{\partial \phi_a}{\partial m_b}\nabla^2 m_b - \left(1 - \left\langle (\vec{\nabla} m)^2 \right\rangle\right) \nabla_m^2 \phi_a \ . \tag{33}$$

Finally, one would like to eliminate the explicit dependence of this equation on $\vec{\phi}(\vec{m})$. Once again, BH exploit the expected insensitivity of the scaling functions to the details of the potential, by choosing the function $\vec{\phi}(\vec{m})$ to satisfy

$$\nabla_m^2 \vec{\phi} \ = \ -\left(\vec{m} \cdot \vec{\nabla}_m\right) \vec{\phi} \ = \ -\sum_b m_b \frac{\partial \vec{\phi}}{\partial m_b} \ , \tag{34}$$

a direct generalization of (7). Substituting the radially symmetric form (29) in (34) gives

$$g'' + \left(\frac{n-1}{\rho} + \rho\right) g' - \frac{n-1}{\rho^2} g \ = \ 0 \ , \tag{35}$$

the equation for the profile function $g(\rho)$ with boundary conditions (30), which generalizes (7). For small ρ the solution is linear,

$$g(\rho) \sim \rho \qquad (\rho \to 0) \ , \tag{36}$$

while for large ρ the profile saturates as

$$g(\rho) \ \simeq \ 1 - (n-1)/2\rho^2 \qquad (\rho \to \infty) \ , \tag{37}$$

from which we can take $\zeta^2 = (n-1)/2$ as a definition of the defect core size. The potential $V(\phi)$ corresponding to this choice of the profile function can be deduced from (28), though it seems unlikely that a closed-form expression can be derived.

With the choice (34), Eq. (33) now becomes

$$\left(\frac{\partial \vec{m}}{\partial t} - \nabla^2 \vec{m} - a(t)\vec{m}\right) \cdot \vec{\nabla}_m \phi_a \;=\; 0 \;, \tag{38}$$

where $a(t)$ is given by (14). Let us define the vector

$$\vec{\Omega} \;\equiv\; \partial \vec{m}/\partial t - \nabla^2 \vec{m} - a(t)\vec{m} \;. \tag{39}$$

In principle, Eq. (38) allows for solutions where $\vec{\Omega}$ and $\vec{\nabla}_m \phi_a$ are orthogonal vectors without $\vec{\Omega}$ being zero. However, inserting the radial form (29) in (38) gives

$$\left(\vec{\Omega} \cdot \vec{\nabla}_m\right) \vec{\phi} \;=\; \frac{g(\rho)}{\rho}\, \vec{\Omega}_\perp + g'(\rho)\, \vec{\Omega}_\parallel \;=\; \vec{0} \;, \tag{40}$$

where $\vec{\Omega}_\perp$ and $\vec{\Omega}_\parallel$ are the components of $\vec{\Omega}$ perpendicular and parallel to $\hat{\vec{m}}$, i.e.,

$$\begin{aligned} \vec{\Omega}_\perp &= \vec{\Omega} - \left(\vec{\Omega} \cdot \hat{\vec{m}}\right) \hat{\vec{m}} \;, \\ \vec{\Omega}_\parallel &= \left(\vec{\Omega} \cdot \hat{\vec{m}}\right) \hat{\vec{m}} \;. \end{aligned} \tag{41}$$

The coefficients g' and g/ρ in (40) only vanish for $\rho \to \infty$, so the orthogonal vectors $\vec{\Omega}_\perp$ and $\vec{\Omega}_\parallel$ must vanish separately everywhere. Therefore $\vec{\Omega} = \vec{0}$ is the only physical solution of (38). Then Eq. (31) reduces to the self-consistent linear form (13) and (14), holding separately for each component of $\vec{m}$. Taking Gaussian initial conditions for each component, with zero mean and correlator (15), the usual procedure leads to the same asymptotic form (24) for the correlator $\langle m_a(1) m_a(2) \rangle$ $(a = 1, ..., n)$, and thus to the same form (26) for the normalized correlator

$$\gamma(1,2) \equiv \frac{\langle \vec{m}(1) \cdot \vec{m}(2) \rangle}{\sqrt{\langle \vec{m}(1)^2 \rangle \, \langle \vec{m}(2)^2 \rangle}} \;. \tag{42}$$

The final step is to evaluate the pair correlation function $C(1,2) = \left\langle \vec{\phi}(1) \cdot \vec{\phi}(2) \right\rangle$. This proceeds exactly as in the BPT treatment [7]: from (25) ρ scales as $\sqrt{t}$, then according to (29) and (30) we can replace the profile $g(\rho)$ by 1 and the function $\vec{\phi}(\vec{m})$ by $\hat{\vec{m}}$ at late times. Since from (13) the components of $\vec{m}$ are Gaussian fields at all times, the calculation of the average $C(1,2) = \left\langle \hat{\vec{m}}(1) \cdot \hat{\vec{m}}(2) \right\rangle$ leads to the standard BPT scaling function [7] (see also the Appendix)

$$\begin{aligned} C(1,2) = \frac{n\gamma}{2\pi} \left[B\left(\frac{n+1}{2}, \frac{1}{2}\right) \right]^2 \\ \times {}_2F_1\left[\frac{1}{2}, \frac{1}{2}; \frac{n+2}{2}; \gamma(1,2)^2\right] \;, \end{aligned} \tag{43}$$

where $B(x,y)$ is the beta function and ${}_2F_1[a,b;c;z]$ is the hypergeometric function.

Remarks similar to those of the previous section, regarding the possibility of systematically improving the results by expanding in $1/N$, apply here. In addition, the present (leading order) results are expected to become exact both for large d and for large n, when the linearization of the $\vec{m}$ equation, leading to the Gaussian property of $\vec{m}$, is justified.

III. OFF-CRITICAL QUENCHES

In the last section we discussed in detail the systematic approach for the $O(n)$ model representing a system undergoing a "critical quench." A remarkable feature of this approach is that it can be extended in a simple manner to treat the situation when an external field is present and/or the initial state contains a bias.

Regarding the external field, the key point of the approach is to select a convenient effective driving force which simplifies the equation for $\vec{m}(\mathbf{r}, t)$ and which captures the essential physics of the problem. To achieve this, we focus on the relevant effect of the external field in the asymptotic dynamics of the ordering system, which is different for scalar and vector systems. The initial bias, on the other hand, only enters the equation for $\vec{m}$ through the initial condition. To leading order in the systematic approach, we obtain a linear equation for the auxiliary field similar to the critical case, but with an extra driving force h for $n = 1$ and $\sqrt{\langle m^2 \rangle}\, \vec{h}$ for $n > 1$. To evaluate the expectation values associated with the order parameter (including $\left\langle \vec{\phi} \right\rangle$, which was zero in the critical case), we extend the Gaussian calculations for a distribution centered about a nonzero average. In particular, we derive the off-critical extension of the BPT scaling function (43).

A. Scalar fields

Our starting point for a nonconserved, scalar system in the presence of an external field is the usual TDGL equation (3), but now the potential $V(\phi)$ is asymmetric.

The energy density due to an external field (e.g., a magnetic field) can be modeled by a linear term coupling the field to the order parameter, which biases the order parameter in the direction of the field. Hence the potential $V(\phi)$ has the form

$$V(\phi; h) = V_0(\phi) - h(t)\, \phi \;, \tag{44}$$

where $V_0(\phi)$ is the usual symmetric, double-well potential, and $h(t)$ is a general time-dependent external field. For a spin system, for example, the above linear form only holds if ϕ is far from saturation and h is not too large, otherwise the system will respond nonlinearly to the field and terms such as $O(h\phi^3)$ become important. In the present continuous order parameter system, the saturation values of ϕ simply get modified by h. For positive h and given t, the potential $V(\phi; h)$ has an asymmetric double-well form, with the right- (left-)hand minimum lower (higher) than in $V_0(\phi)$. For our purposes, it is convenient to rewrite the potential in the generic form

$$V(\phi; h) = V_0(\phi) - h(t)\, V_1(\phi) \;, \tag{45}$$

where $V_1(\phi)$ is a monotonic, odd function of ϕ. Then the evolution equation for the order parameter reads

$$\frac{\partial \phi}{\partial t} = \nabla^2 \phi - V_0'(\phi) + h(t)\, V_1'(\phi) \;. \tag{46}$$

As in the treatment of the case $h = 0$, we can exploit

the insensitivity of the domain growth to specific details of the potential by choosing an especially convenient form for $V(\phi)$. This relies on the physical idea that the interface motion only depends on the local curvature K and on the local field h. To motivate this idea, we derive the generalized version of Allen-Cahn's equation for the interface motion, valid for an arbitrary potential. If g is a coordinate normal to the interface (increasing in the direction of increasing ϕ), the TDGL equation (3) can be recast near an interface as

$$-\left(\frac{\partial\phi}{\partial g}\right)_t\left(\frac{\partial g}{\partial t}\right)_\phi = K\left(\frac{\partial\phi}{\partial g}\right)_t + \left(\frac{\partial^2\phi}{\partial g^2}\right)_t - V'(\phi)\ , \tag{47}$$

where the curvature K is the divergence of the "outward" normal (i.e., pointing in the direction of increasing ϕ) to the interface. Multiplying through by $(\partial\phi/\partial g)_t$ and integrating over g through the interface gives the local velocity of the interface, $v = (\partial g/\partial t)_\phi$, as

$$v = -K + \Delta V/\Sigma\ , \tag{48}$$

where ΔV is the change in the potential $V(\phi, h)$ across the interface and $\Sigma = \int dg(\partial\phi/\partial g)_t^2$ is the surface tension. The essential point here is that the interface motion depends on the external field only through ΔV. So, as far as domain growth is concerned, all that matters is the difference between the minima of the potential $V(\phi; h)$ for the two bulk phases. This gives us a great deal of flexibility in the choice of $V_1(\phi)$. In particular, we may choose the minima of $V(\phi; h)$ to remain at $\phi = \pm 1$, avoiding inessential contributions to the magnetization from "stretching" the field.

As usual, we introduce the auxiliary variable $m(\mathbf{r}, t)$ whose zeros determine the wall positions. Rewriting Eq. (46) in terms of m yields

$$\phi'\dot{m} = \phi'\nabla^2 m + \phi''(\vec{\nabla}m)^2 - V_0'(\phi) + h(t)V_1'(\phi)\ . \tag{49}$$

We define the transformation $\phi = \phi(m)$ by the equilibrium wall profile for the asymmetric potential. This situation corresponds to a planar moving wall (moving, say, in the positive x direction) with position $x_0(t)$ and velocity $v(t) = \dot{x}_0(t)$. So, the equilibrium solution is of the form

$$\phi(\mathbf{r}, t) = \phi(x - x_0(t))\ . \tag{50}$$

Substituting this in (46) gives the equation for the steady-state profile

$$\begin{aligned} V'(\phi; h) &= \phi''(m) + v(t)\,\phi'(m) \\ &= V_0'(\phi) - h(t)V_1'(\phi)\ , \end{aligned} \tag{51}$$

which generalizes (4), and has the same boundary conditions (5). This immediately suggests the convenient choices

$$V_0'(\phi) = \phi''(m)\ , \tag{52}$$

$$V_1'(\phi) = \phi'(m)\ , \tag{53}$$

along with the identification

$$v(t) = -h(t)\ . \tag{54}$$

Note that (52) determines the profile for a given $V_0(\phi)$, or vice versa, while (53) fixes $V_1(\phi)$ for a given profile $\phi(m)$. In addition, we adopt the BH choice (7) for the function $\phi(m)$, i.e., $\phi'' = -m\,\phi'$. Inserting (52), (53), and (7) in (49), we obtain the simpler equation

$$\dot{m} = \nabla^2 m + \left[1 - (\nabla m)^2\right]\, m + h(t)\ . \tag{55}$$

The condition (7) gives once again the error function profile (8), and amounts, via (52), to choosing the previous form (10) for the symmetric potential $V_0(\phi)$. The potential $V_1(\phi)$ is obtained by integrating (53), with boundary condition $V_1(0) = 0$. This gives

$$\begin{aligned} V_1(\phi) = \int_0^m dx\ [\phi'(x)]^2 &= \frac{2}{\pi}\int_0^m dx\ \exp\left(-x^2\right) \\ &= \frac{1}{\sqrt{\pi}}\mathrm{erf}(m) \qquad (56) \\ &= \frac{1}{\sqrt{\pi}}\mathrm{erf}\left[\sqrt{2}\mathrm{erf}^{-1}(\phi)\right] \qquad (57) \end{aligned}$$

where we used (8). Alternatively, from (53) and (9), we get

$$V_1(\phi) = \int_0^\phi dx\,\sqrt{2V_0(x)}\ . \tag{58}$$

Again, (57) or (58) only defines $V_1(\phi)$ for $\phi^2 \le 1$, but this is the only region we require for $T = 0$. In particular, we have $V_1(\phi) \simeq \sqrt{2/\pi}\,\phi$ for $\phi^2 \ll 1$, while $V_1(\phi) \simeq \pm\left[1/\sqrt{\pi} - (1/4)(1-\phi^2)^2\sqrt{|\ln(1-\phi^2)|/2}\right]$ for $\phi^2 \simeq 1$. Therefore $V_1(\phi)$ has a sigmoid shape, with linear behavior (44) for small ϕ, while saturating to $\pm 1/\sqrt{\pi}$ in the bulk and so acting only on the interfaces. We can relate our field $h(t)$ to an effective field driving the interface dynamics by matching the differences $\Delta V = -2h_{eff}$, which follows from (44), and $\Delta V = -h\Delta V_1 = -2h/\sqrt{\pi}$. This yields $h_{eff} = h/\sqrt{\pi}$. [Alternatively, we can note from (54) that the field h is scaled such that the proportionality constant between the velocity and the field for a flat domain wall is unity.] Note that, if we had kept the form (44) throughout ($V_1' = 1$), the minima of $V(\phi; h)$ would be shifted by the field h, which is inconsistent with the use of the profile function (8), where $\phi^2 \le 1$. This would also give a nonlinear term $h/\phi' \sim \exp(m^2/2)$ in (55), amplifying the effect of the field in the bulk (and thus shifting the minima of V) and destroying the mathematical simplicity of the equations.

Expectation values

In order to solve Eq. (55), we use the replacement (12) for $\left(\vec{\nabla}m\right)^2$, which corresponds to taking the limit $d \to \infty$ or a large number of "colors," N. With this, (55) becomes the self-consistent equation for $m(\mathbf{r}, t)$:

$$\dot{m} = \nabla^2 m + a(t)\, m + h(t)\ , \tag{59}$$

with $a(t)$ given by (14); a simple extension of (13). In addition, we allow for a uniform bias in the initial state,

taking Gaussian initial conditions for m with nonzero mean, and only short-ranged correlations

$$\langle m(\mathbf{r},0)\rangle = m_0 \ , \tag{60}$$

$$\begin{aligned}\langle m(\mathbf{r},0)m(\mathbf{0},0)\rangle_c &\equiv \langle m(\mathbf{r},0)m(\mathbf{0},0)\rangle - \langle m(\mathbf{r},0)\rangle^2 \\ &= \Delta\delta(\mathbf{r}) \ .\end{aligned} \tag{61}$$

The Fourier components of $m(\mathbf{r},\mathbf{0})$ still satisfy $\langle m_{\mathbf{k}}(0)\rangle = 0$ and (15) for $\mathbf{k} \neq \mathbf{0}$.

Solving Eq. (59) in Fourier space gives

$$\begin{aligned}m_{\mathbf{k}}(t) = m_{\mathbf{k}}(0)\, &\exp\left[-k^2 t + b(t)\right] \\ &+(2\pi)^d \delta(k) \int_0^t dt'\, h(t')\, \frac{\exp[b(t)]}{\exp[b(t')]} \ ,\end{aligned} \tag{62}$$

with $b(t)$ defined by (17). Since $\left\langle (\vec{\nabla} m)^2 \right\rangle$ is unaffected by the presence of a uniform bias and field, it is the same as for $h = 0 = m_0$. Hence the function $b(t)$ is still determined by the self-consistency equation (18), leading once again to the asymptotic form (19) for times $t \gg t_0$, with t_0 given by (20). Inserting this result in (62) yields, for large t,

$$\begin{aligned}m_{\mathbf{k}}(t) = (t/t_0)^{\frac{d+2}{4}} \Big\{ &m_{\mathbf{k}}(0)\, \exp\left(-k^2 t\right) \\ &+(2\pi)^d \delta(\mathbf{k})\, \eta(t) \Big\} \ ,\end{aligned} \tag{63}$$

with

$$\eta(t) = \int_{t_0}^t dt'\, h(t') \left(\frac{t_0}{t'}\right)^{\frac{d+2}{4}} \ , \tag{64}$$

where the lower cutoff t_0 was introduced into the integral to account for the breakdown of the form used for $b(t)$ at short times. Although the form used for $b(t)$ is only valid in the scaling regime ($t \gg t_0$) we shall be taking $t \geq t_0$ for computational convenience. This gives an inaccurate description of the initial transient behavior prior to the scaling regime, but is irrelevant for the scaling behavior [for more details see the discussion following (21)].

Averaging (63) over initial conditions and taking the Fourier transform gives the average value of $m(\mathbf{r},t)$ at late times

$$\langle m(t)\rangle = (t/t_0)^{\frac{d+2}{4}} \left[m_0 + \eta(t)\right] \ . \tag{65}$$

From (63) we also obtain the previous expressions, (24) and (25), for the second cumulants of m, i.e., the connected pair correlator and one-point correlator:

$$\begin{aligned}C_0(1,2) &\equiv \langle m(1)m(2)\rangle_c \\ &= \langle m(1)m(2)\rangle - \langle m(1)\rangle \langle m(2)\rangle \ ,\end{aligned} \tag{66}$$

$$S_0(t) \equiv \langle m^2\rangle_c = \langle m^2\rangle - \langle m\rangle^2 \ . \tag{67}$$

This immediately gives the same form (26) for the off-critical normalized correlator

$$\begin{aligned}\gamma(1,2) &\equiv \frac{\langle m(1)m(2)\rangle_c}{\sqrt{\langle m(1)^2\rangle_c \langle m(2)^2\rangle_c}} \\ &= \left(\frac{4t_1 t_2}{(t_1+t_2)^2}\right)^{d/4} \exp\left(-\frac{r^2}{4(t_1+t_2)}\right) \ .\end{aligned} \tag{68}$$

For equal times ($t_1 = t_2 = t$), (68) simplifies to

$$\gamma(1,2) = \exp\left(-\frac{r^2}{8t}\right) \ . \tag{69}$$

As usual, at late times we can replace the profile function $\phi(m)$ [Eq. (8)] by $\mathrm{sgn}(m)$ to evaluate the expectation values associated with the field ϕ. According to (59), $m(\mathbf{r},t)$ is a Gaussian field at all times, with probability distribution defined by the nonzero mean (65) and the second cumulants (67) and (67). Evaluating the Gaussian expectation values, we obtain scaling functions with arguments (65), (67) and (68). The details of these calculations are given in the Appendix, so we shall state the results only.

Magnetization

For the average value of the order parameter ϕ, i.e., the magnetization, we obtain

$$\langle \phi(t)\rangle = \langle \mathrm{sgn}(m)\rangle = \mathrm{erf}\left[M(t)\right] \ , \tag{70}$$

where $M(t)$ is a dimensionless average of m:

$$M(t) \equiv \frac{\langle m\rangle}{2\sqrt{\langle m^2\rangle_c}} \tag{71}$$

$$= \sqrt{d/8t_0} \left(\frac{t}{t_0}\right)^{d/4} \left[m_0 + \eta(t)\right] \ . \tag{72}$$

Some results for $\langle \phi(t)\rangle$ are presented in Figs. 1 and 2. The result using the profile (8) is $\langle \phi\rangle = \mathrm{erf}\left[M/(1+\zeta^2/2\langle m^2\rangle_c)^{1/2}\right]$, with $\zeta = \sqrt{2}$ the wall width

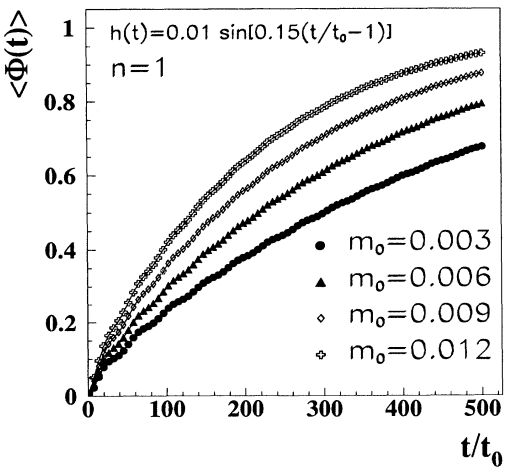

FIG. 1. Magnetization for $d = 3$ and $n = 1$, with a sinusoidal external field $h(t) = 0.01\sin[0.15(t/t_0 - 1)]$ and an initial bias from $m_0 = 0.003$ to $m_0 = 0.012$. Note that $\langle \phi(t_0)\rangle > 0$.

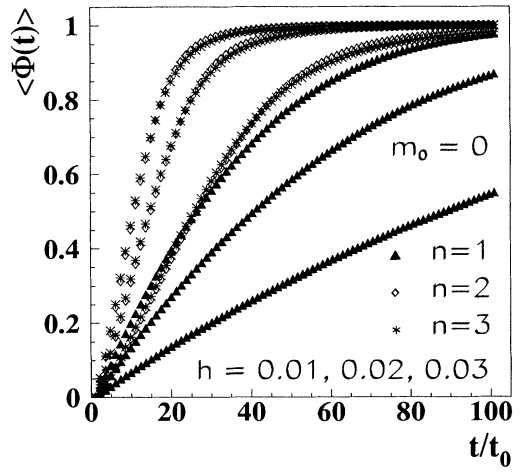

FIG. 2. Magnetization for $d = 3$ and $n = 1, 2, 3$, with a constant external field $h = 0.01, 0.02, 0.03$ (bottom to top) and initial bias $m_0 = 0$.

for this profile. Clearly this reduces to (70) in the scaling regime. In the saturation limit ($|M| \to \infty$) we expand the error function in (70) to give

$$\langle \phi(t) \rangle \simeq \mathrm{sgn}[M(t)] \left[1 - \frac{\exp\left[-M^2(t)\right]}{|M(t)|\sqrt{\pi}} \right] , \quad |M(t)| \gg 1 , \tag{73}$$

and so the magnetization saturates exponentially fast. Conversely, in the "initial-growth" regime when M is small [e.g., for small m_0 and $h(t)$ and t not too large], (70) reduces to

$$\langle \phi(t) \rangle \simeq (2/\sqrt{\pi})\, M(t), \ |M(t)| \ll 1 , \tag{74}$$

showing that in this limit M plays the role of a magnetization.

The time dependence of $\langle \phi \rangle$ is determined by the spatial dimension d. On one hand there is the prefactor $t^{d/4}$ in M. On the other hand note that M has two contributions with different physical origins: one comes from the initial bias while the other is due to the external field. Which term dominates at late times ($t \gg t_0$) depends on the value of d and on the explicit form of $h(t)$. It is also interesting to note that, if we set $h(t)$ to vanish over a time $t_1 > t_0$, then

$$M(t) = (t/t_1)^{d/4}\, M(t_1) , \tag{75}$$

i.e., the "magnetization" induced at subsequent times grows in the same manner as the one induced by the initial bias. To illustrate the nature of the interplay between the magnetization growth induced by the initial bias and that driven by the external field, let us consider a time-independent field h. In this case (64) reduces to

$$\eta(t) = h \int_{t_0}^{t} dt' \, (t_0/t')^{\frac{d+2}{4}} \tag{76}$$

$$\begin{aligned} &= A\, h t_0 \left\{ (t/t_0)^{\frac{2-d}{4}} - 1 \right\} \sim h\,(t/t_0)^{\frac{2-d}{4}} , \quad d < 2 \\ &= h t_0 \ln(t/t_0), \quad d = 2 \\ &= A\, h t_0 \left\{ 1 - (t_0/t)^{\frac{d-2}{4}} \right\} \sim h, \quad d > 2 , \end{aligned} \tag{77}$$

where $A = 4/|d-2|$. The asymptotic forms on the right stand for late times $t \gg t_0$. For $d \leq 2$ the integral (76) is dominated by times of order t, so the continued influence of the field dominates over the initial bias in (72) at late times. For $d > 2$ the integral is dominated by short times, so $\eta(t)$ scales like the initial bias m_0 in (72). This means that the prevalent effect of the field is the growth induced at early times, a similar situation to that described by (75). For a general time-dependent field $h(t)$ the crossover between these two regimes will be different, but clearly the factor $1/t'^{(d+2)/4}$ in (64) diminishes the effect of the field as time progresses. In particular, a sinusoidal field is less effective in reversing the magnetization during later cycles. This situation is illustrated in Fig. 1.

Using linear response and scaling arguments BK [12] predicted the scaling form of the magnetization in the "initial-growth" regime when $\langle \phi \rangle \ll 1$. Our expression (74)–(76) for $\langle \phi \rangle$ agrees closely with their scaling form. The essential modification is that $t^{d/4} = L^{d/2}$ gets replaced by L^{λ}, where $\bar{\lambda} = d - \lambda$ is the exponent characterizing the decay of the autocorrelation function. Hence the crossover between the two regimes no longer occurs at $d = 2$ but at the dimension where $\lambda = 1$ [12]. In the systematic approach, as in the OJK theory, the exponent λ is given by

$$\lambda_{SA} = d/2 . \tag{78}$$

The BK scaling prediction provides a means of measuring λ without having to measure correlations between fields at different times. The result (70), although approximate, provides an explicit expression for the magnetization, describing the complete time range from the early scaling regime to final saturation ($\langle \phi \rangle \to \pm 1$).

To conclude this discussion, we address the situation when the initial bias m_0 and the constant field h have opposite signs. According to (77) and (72) the magnetization is reversed after a time t_{rev} given by

$$\begin{aligned} (t_{rev}/t_0)^{\frac{2-d}{4}} &= 1 + |m_0|/|h t_0\, A| \quad \text{for} \quad d < 2 , \\ t_{rev}/t_0 &= \exp\left(|m_0|/|h t_0|\right) \quad \text{for} \quad d = 2 . \end{aligned} \tag{79}$$

For $d > 2$, however, a sufficiently weak field $|h| < |m_0|/A t_0$ can never overpower the initial bias and the system evolves towards the metastable state corresponding to $\langle \phi \rangle = \mathrm{sgn}(m_0)$. This result is for a system at zero temperature (there is no noise in the equation of motion). At temperatures $T > 0$ thermal fluctuations will eventually drive the system towards stable equilibrium [corresponding to $\langle \phi \rangle = \mathrm{sgn}(h)$] for any d. Does the above statement agree with what we should expect for $T = 0$? We recall

the two effects of the magnetic field. Initially it creates a bias which grows in the same manner as the bulk magnetization induced by m_0 [Eq. (75)]; the net result is the sum of these two. In addition it produces a wall driving force which adds to the wall curvature force (which exists for $d > 1$) [16]. The net force dictates which of the two effects dominates at late times. Within our approach the curvature dominates for $d > 2$ (but not for $d \leq 2$), in which case the magnetization is determined by the net bias growth, i.e., the balance between m_0 and h. We would expect the curvature to dominate for any $d > 1$ when the field h is small enough, but we cannot say precisely, within this qualitative argument, how small h should be compared to m_0. The results for $1 < d \leq 2$ are probably an artifact of the approach, which is in fact a large-d treatment. Therefore the behavior found for $d > 2$ is probably the only physical behavior when $d > 1$ and h is very small.

Pair correlations

For the pair correlation function of the field ϕ, we obtain (see the Appendix)

$$C(1,2) = \langle \mathrm{sgn}[m(1)]\mathrm{sgn}[m(2)] \rangle = \frac{2}{\pi} \int_0^{\gamma(1,2)} \frac{dy}{\sqrt{1-y^2}} \exp\left[-\Gamma(y)\right] + \langle\phi(1)\rangle\langle\phi(2)\rangle \ , \tag{80}$$

with

$$\Gamma(y) = \frac{M^2(1) + M^2(2) - 2yM(1)M(2)}{1-y^2} \ , \tag{81}$$

where $M(i) = M(t_i)$ is given by (72) and $\gamma(1,2)$ is given by (68). In the critical limit ($m_0 = h = 0$) we have $M = \langle\phi\rangle = 0$, hence the usual OJK form $C = (2/\pi)\sin^{-1}\gamma$ is recovered. For widely separated times ($t_2/t_1 \to \infty$) or for infinitely separated points ($r \to \infty$), we have $\gamma \to 0$, and so $C(1,2) \to \langle\phi(1)\rangle\langle\phi(2)\rangle$.

At equal times [$M(1) = M(2) = M(t)$], (80) reduces to

$$C(x,M) = \frac{2}{\pi} \int_0^{\gamma(x)} \frac{dy}{\sqrt{1-y^2}} \exp\left(\frac{-2M^2}{1+y}\right) + \langle\phi\rangle^2 \tag{82}$$

$$= 1 - \frac{2}{\pi} \int_{\gamma(x)}^{1} \frac{dy}{\sqrt{1-y^2}} \exp\left(\frac{-2M^2}{1+y}\right) \ , \tag{83}$$

where $x = r/t^{1/2}$ is the scaling variable and $\gamma(x)$ is given by (69). It is worth studying the limiting behavior of this expression. For $\gamma \to 1$ ($x \to 0$) one obtains, to leading order in x,

$$C(x,M) = 1 - \exp\left[-M^2(t)\right]\ \left[(1/\pi)x + O(x^3)\right] \qquad x \to 0 \ . \tag{84}$$

Note that the term $\exp[-M^2(t)]\,x$ is, up to constants, $\rho_{def}(t)\,r$, where ρ_{def} is the wall density, given by (88) below. This shows that the correlation function $C(x,M)$ has a small-distance Porod's regime, as expected. In the limit $\gamma \to 0$ ($x \to \infty$), we take $r \to \infty$ keeping t fixed in order to have $M(t)$ fixed. Then, Taylor expanding (82) we obtain

$$C(x,M) = \frac{2}{\pi} \exp\left[-2M^2(t)\right]\ \left[\gamma + M(t)^2\gamma^2 + \cdots\right] + \langle\phi\rangle^2 \quad , \quad x \to \infty \ . \tag{85}$$

In the saturation limit, when $M(t)^2 \to \infty$ and $\langle\phi\rangle^2 \to 1$, $C(x,t)$ saturates exponentially to 1 in (83)–(85). The equal-time pair correlation scaling function $C(x,M)$ is shown in Fig. 3, for a constant external field.

Density of walls

We are also interested in the average density of wall "area" per unit volume of the system, $\rho_{def}(t)$. There are a number of ways of calculating ρ_{def} within the Gaussian approximation. For example, $\rho_{def} = \left\langle (\nabla\phi)^2 \right\rangle / \Sigma = -\left(\nabla^2 C\right)_{r=\zeta} / \Sigma$, where Σ is the surface tension, can be evaluated from (83). The results differ by a constant amplitude, as a consequence of the inaccuracy of the approximation, but our main interest is to obtain the time dependence of the wall density. A simple procedure [17, 18] which easily generalizes for vector fields is to write the wall density at each point $\mathbf{r}$ in terms of the auxiliary field m as

$$\rho_{def}(\mathbf{r},t) = \delta(m(\mathbf{r},t))\,|\vec{\nabla} m(\mathbf{r},t)| \ , \tag{86}$$

where $|\nabla m|$ is the Jacobian between m and the spatial coordinate $\mathbf{r}$. If we adopt the usual definition of m as a normal coordinate near defects, then $|\nabla m| = 1$ at defects, giving simply $\rho(\mathbf{r},t) = \delta(m(\mathbf{r},t))$ [17] (note that this is true for the exact m, but not for the Gaussian m, for which $|\vec{\nabla} m|$ fluctuates). Now we make the

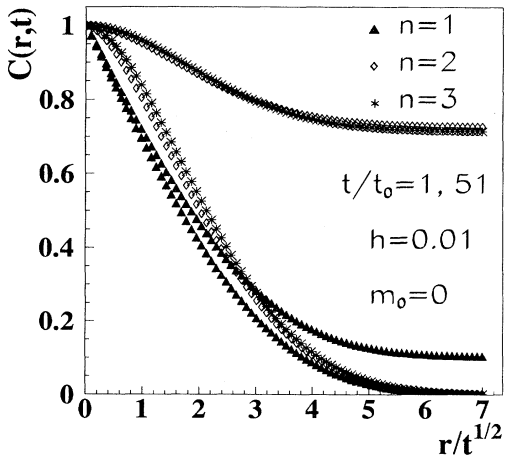

FIG. 3. Equal-time pair correlation function for $d = 3$, $n = 1, 2, 3$, and at times $t/t_0 = 1, 51$, with a constant external field $h = 0.01$ and initial bias $m_0 = 0$. The behavior at large r is described by (128).

Gaussian approximation for m with the one-point distribution function

$$P(m) = \frac{1}{\sqrt{2\pi S_0}} \exp\left(\frac{-(m-\langle m\rangle)^2}{2S_0}\right) . \quad (87)$$

Then the average wall density is given by

$$\rho_{def}(t) = \langle \delta(m)\rangle = P(0) = \sqrt{\frac{d}{8\pi}} \frac{\exp\left[-M^2(t)\right]}{\sqrt{t}} , \quad (88)$$

where we used (25), and $M(t)$ is given by (72). This result agrees, up to constants, with an earlier prediction by OJK [3]. When $m_0 = h = 0$, (88) gives the usual scaling form $\rho \sim L^{d-1}/L^d \sim 1/L$. The ordering process is much faster in the presence of an external field or initial bias, hence the exponential decay of the wall density.

B. Vector fields

The evolution of a nonconserved vector system in the presence of an external field is given by the TDGL equation (2). The usual form of the potential $V(\vec{\phi})$ (for "soft spins") is a direct generalization of (44), i.e.,

$$V(\vec{\phi};\vec{h}) = V_0(\vec{\phi}) - \vec{h}(t)\cdot\vec{\phi} , \quad (89)$$

where $V_0(\vec{\phi})$ is the usual sombrero potential, with a symmetric ground state manifold $\vec{\phi}^2 = 1$, and $\vec{h}(t)$ is a general time-dependent external field. The full potential $V(\vec{\phi};\vec{h})$ has an asymmetric (tilted) sombrero shape, with a single global minimum where $\vec{\phi}$ is parallel to $\vec{h}$ and has maximum length (among all the minima), and an unstable state where $\vec{\phi}$ is antiparallel to $\vec{h}$ and has minimum length. These saturation lengths depend on the value of $|\vec{h}|$. For the remaining directions of $\vec{\phi}$ there is only a minimum along each direction, corresponding to a local saturation length, which varies continuously between the two above values.

As usual for vector systems, we want to introduce a vector auxiliary field $\vec{m}$ whose zeros define the locations of the topological defect cores. By analogy with the previous cases, in order to define the transformation $\vec{\phi}(\vec{m})$ let us imagine what a steady-state configuration of the field $\vec{\phi}$ looks like in the presence of a slowly varying field $\vec{h}$. For definiteness consider a system with $n = d$, which has point topological defects (i.e., vortices for $d = 2$ and monopoles for $d = 3$), along with antidefects. These attract each other and eventually annihilate at late times. Without an external field the defects are radially symmetric: at the defect core $\vec{\phi}$ has zero length and undefined direction, while away from the defect core $\vec{\phi}$ rapidly saturates in length. The effect of the field $\vec{h}$ is to deform the defects: all "force lines" (except one) emerging from the defect core tend to line up with $\vec{h}$ away from the core. Close enough to the defect core, however, the field $\vec{\phi}$ will still be isotropic, so we may still use the "radially symmetric" form (29), i.e.,

$$\vec{\phi}(\vec{m}) = g(\rho)\,\hat{\vec{m}} , \quad (90)$$

where $\rho = |\vec{m}|$ and $g(\rho)$ is a function yet to be determined. In the vicinity of a core, where $\hat{\vec{m}}$ is isotropic, ρ and $g(\rho)$ play the same role as in the case $\vec{h} = \vec{0}$, while in the bulk the direction of $\hat{\vec{m}}$ is (on average) parallel to $\vec{h}$. Note that, by symmetry, there is no direct force on the defect core due to the external field.

Contrary to the scalar case, we conclude that an important effect of the external field occurs in the bulk, where the relevant phenomenon is the orientational ordering of $\vec{\phi}$ along the direction of $\vec{h}$. In the bulk we expect $\vec{\phi}$ to rapidly relax to its saturation length, i.e., to the "local" minimum of $V(\vec{\phi};\vec{h})$ which depends on the local angle between $\vec{\phi}$ and $\vec{h}$. In other words, since field "stretching" is a local process while field rotation involves long-range correlations, the longitudinal effect of $\vec{h}$ (along $\vec{\phi}$) should be instantaneous as compared to transverse effects. The same assumption has motivated large-n studies of this problem using a "hard-spin" model [19, 12]. This leads us to interpret $g(\rho)$ in (90) as the *stationary* profile function of a defect in the field $\vec{\phi}$, with $|\vec{m}|$ representing the distance from the defect along a (time-dependent) "force line" defined by $\hat{\vec{m}}$. Hence, as far as bulk rotation and the slow defect dynamics are concerned, we may once again (but for reasons different from the scalar case) ignore the inessential "stretching" of the field, by choosing the local minima of $V(\vec{\phi};\vec{h})$ to remain at $\vec{\phi}^2 = 1$. This amounts to taking the same boundary conditions (30) for $g(\rho)$.

With these insights, let us rewrite the TDGL equation (2) as

$$\frac{\partial\vec{\phi}}{\partial t} = \nabla^2\vec{\phi} - \frac{dV_0(\vec{\phi})}{d\vec{\phi}} + \vec{U}(\vec{\phi};\vec{h}) , \quad (91)$$

where $\vec{U}(\vec{\phi};\vec{h})$ is the driving force due to the field $\vec{h}$ [which would be simply $\vec{h}$ with the potential (89)]. As usual, we expect the scaling functions to be insensitive to the details of the potential, or equivalently of the driving force. These should only affect phenomena on the scale of the defect core size ζ, but not on the scale of the bulk characteristic length $L(t)$. Thus we can make convenient choices for V_0 and $\vec{U}$ in order to simplify the equation of motion for $\vec{m}$.

As in the case $\vec{h} = \vec{0}$, we define the relation between the function $\vec{\phi}(\vec{m})$ and the potential $V_0(\vec{\phi})$ by Eq. (28). Rewriting (91) in terms of $\vec{m}$ gives (31) but with an extra term U_a. As usual, we use the replacement (32) which is justified in the large-n limit, where $\left\langle(\vec{\nabla}m)^2\right\rangle$ still stands for any component of $\vec{m}$. Note that $(\vec{\nabla}m)^2$ is unaffected by a *uniform* external field or bias, so the system is isotropic as far as the average $\left\langle(\vec{\nabla}m)^2\right\rangle$ is concerned. We also choose the function $\vec{\phi}(\vec{m})$ to satisfy (34). This leads once again, via (90), to Eq. (35) for the profile function $g(\rho)$, with small- and large-ρ behavior (36) and (37). It also corresponds to the same choice for the symmetric potential $V_0(\vec{\phi})$ as in the case $\vec{h} = \vec{0}$. Putting it all

together and using definition (39), the TDGL equation (91) then becomes

$$\left(\vec{\Omega}\cdot\vec{\nabla}_m\right)\vec{\phi} = \vec{U}(\vec{\phi};\vec{h}) \ . \tag{92}$$

The key step now is to rewrite the driving force in the anisotropic form

$$\vec{U}(\vec{\phi};\vec{h}) = U_\perp(g)\,\vec{h}_\perp + U_\parallel(g)\,\vec{h}_\parallel \ , \tag{93}$$

and to use (90) to write the left-hand side of (92) as in (40), i.e., as

$$\left(\vec{\Omega}\cdot\vec{\nabla}_m\right)\vec{\phi} = \frac{g(\rho)}{\rho}\,\vec{\Omega}_\perp + g'(\rho)\,\vec{\Omega}_\parallel \ , \tag{94}$$

where the indices $\parallel$ and $\perp$ refer to the components of the vectors parallel and perpendicular to $\vec{\phi}$ [Eq. (41)]. Matching (93) and (94) gives immediately

$$\begin{aligned}\Omega_\perp(\vec{m}) &= \frac{\rho}{g(\rho)}\,h_\perp\,U_\perp \ , \\ \Omega_\parallel(\vec{m}) &= \frac{1}{g'(\rho)}\,h_\parallel\,U_\parallel \ .\end{aligned} \tag{95}$$

To obtain a simple, "isotropic" equation of motion for $\vec{m}$, we adopt the following choice for the driving force:

$$\begin{aligned}U_\perp &= g(\rho) \ , \\ U_\parallel &= \rho\,g'(\rho) \ .\end{aligned} \tag{96}$$

This corresponds, via (93), (36), and (37), to having

$$\begin{aligned}&\vec{U} \sim \rho\,\vec{h} \qquad (\rho \to 0) \ , \\ &\vec{U} \simeq \vec{h}_\perp \ + \ (1-\vec{\phi}^2)\left(\vec{h}_\parallel - \vec{h}_\perp/2\right) \qquad (\rho \to \infty) \ ,\end{aligned} \tag{97}$$

in total agreement with the requirements from the above discussion: $\vec{U}$ vanishes at the defect cores, while being isotropic in their vicinity; in the bulk $\vec{U}$ reduces to its transverse component, forcing $\vec{\phi}$ to rotate and to line up with $\vec{h}$. Just as in the scalar case, the driving force derives from a potential $\vec{U}(\vec{\phi};\vec{h}) = dV_1(\vec{\phi};\vec{h})/d\vec{\phi}$. To get an equation for V_1 one writes $\vec{U}$ in terms of $\vec{\phi}_\parallel$ and $\vec{\phi}_\perp$, the components of $\vec{\phi}$ parallel and perpendicular to $\vec{h}$. However, according to (93) and (96) one cannot deduce V_1 without solving Eq. (35) for $g(\rho)$. Nonetheless, all that matters is the driving force which is physically correct.

Expectation values

We now solve the equation for $\vec{m}$ and obtain its expectation values. With the choice (96) and using definition (39) of $\vec{\Omega}$, the equation of motion (95) becomes

$$\partial\vec{m}/\partial t = \nabla^2\vec{m} + a(t)\,\vec{m} + \rho\,\vec{h}(t) \ . \tag{98}$$

In the spirit of the systematic approach, in order to obtain a linear equation for $\vec{m}$ we replace $\vec{m}^2$ by its average in ρ:

$$\rho = \sqrt{\vec{m}^2} \to \sqrt{\langle\vec{m}^2\rangle} \ , \tag{99}$$

which would be exact in the large-n limit. For convenience we set the external field in the $(1,1,...)$ direction

$$\vec{h}(t) = \frac{h(t)}{\sqrt{n}}\,(1,1,...) \ . \tag{100}$$

Clearly, the scaling functions will not depend on this arbitrary choice. As in the scalar case we also consider an initial state with a uniform bias. For simplicity we restrict the bias to be parallel or antiparallel to the external field:

$$\langle\vec{m}(\mathbf{r},0)\rangle = m_0\,(1,1,...) \ . \tag{101}$$

From (98), (100), and (101) it follows that the different components of $\vec{m}$ have the same expectation values at all times. Hence $\langle\vec{m}\rangle = \langle m\rangle\,(1,1,...)$ and $\langle\vec{m}^2\rangle = n\,\langle m^2\rangle$, where m is any component of $\vec{m}$. Inserting (99) and (100) in (98), we obtain the self-consistent linear equation for the components of $\vec{m}(\mathbf{r},t)$:

$$\partial m/\partial t \ = \ \nabla^2 m + a(t)\,m + c(t)\,h(t) \ , \tag{102}$$

$$\begin{aligned}a(t) &= 1 - \left\langle(\nabla m)^2\right\rangle \ , \\ c(t) &= \sqrt{\langle m^2\rangle} \ = \ \sqrt{S_0(t) + \langle m\rangle^2} \ ,\end{aligned} \tag{103}$$

which is the vector field version of (59).

The calculation of the expectation values of m proceeds as in the previous subsection; the only difference is that $c(t)$, or equivalently $M(t)$ or $\eta(t)$, has to be determined self-consistently whenever $h \neq 0$. As usual we adopt a Gaussian distribution with mean m_0 and second cumulant (61) for the initial condition of each component of $\vec{m}$. Fourier transforming (102), and noting that $b(t)$ [defined by $\dot{b}(t) = a(t)$] is still given by (19) for $t > t_0$, yields the same solution (63) for $m_{\mathbf{k}}(t)$, but where $\eta(t)$ is now given by

$$\eta(t) = \int_{t_0}^{t} dt'\,h(t')\,c(t')\left(\frac{t_0}{t'}\right)^{\frac{d+2}{4}} \ , \tag{104}$$

rather than (64). This leads to the same expressions (65), (24), and (25) for the single-component averages $\langle m\rangle$, $\langle m(1)m(2)\rangle_c$, and $\langle m^2\rangle_c$. Hence the normalized correlator $\gamma(1,2)$ is again given by (68), and the dimensionless average $M(t)$ is given by (72) but with $\eta(t)$ obeying (104). Using (103), (71), and (25) we may rewrite the driving force as $c(t)h(t) = \sqrt{4t/d}\,\sqrt{1+2M^2(t)}\,h(t)$. Inserting this in (104), and then (104) in (72), gives the explicit equation for $M(t)$

$$\begin{aligned}\sqrt{2}M(t) = \left(\frac{t}{t_0}\right)^{d/4}\Bigg[m_0' + \int_{t_0}^{t} dt'\,h(t')\left(\frac{t_0}{t'}\right)^{d/4} \\ \times\sqrt{1+2M^2(t')}\Bigg] \ ,\end{aligned} \tag{105}$$

with $m_0' = \sqrt{d/4}\,m_0/\sqrt{t_0}$. For $h \neq 0$ this is a self-consistent equation which has to be solved numerically. It yields a much faster growth for $M(t)$ than in the scalar case [Eq. (72)], where the integral in (105) is just (64),

i.e., $c(t) = 1$. Alternatively, we could write equations for $c(t)$ or $\eta(t)$, but $M(t)$ is the relevant quantity for the scaling functions. Equation (105) may be recast in the differential form

$$\frac{d}{dt}\left(\frac{\sqrt{2}M}{t^{d/4}}\right) = h(t)\sqrt{\frac{1}{t^{d/2}} + \left(\frac{\sqrt{2}M}{t^{d/4}}\right)^2} , \qquad (106)$$

with initial condition at $t = t_0$

$$\left(\frac{\sqrt{2}M}{t^{d/4}}\right) = \frac{m_0'}{t_0^{d/4}} \quad , \quad t = t_0 . \qquad (107)$$

This is equivalent to the equation obtained by BK [12] in the large-n treatment of the dynamics of $\vec{\phi}$.

As suggested by (106), we find that M is a scaling function of t and $h(t)$. To show this it is convenient to separate the cases $h = \text{const}$ and $h = h(t)$. First we consider a time-independent external field h. Without loss of generality we set $h > 0$, while allowing the initial bias to be $m_0 > 0$ or $m_0 < 0$. Defining the scaling function and variables

$$N(y,z) = \sqrt{2}M(t)/y^{d/4} , \qquad (108)$$

$$y = ht , \qquad (109)$$

$$z = m_0'/(ht_0)^{d/4} = m_0'/y_0^{d/4} , \qquad (110)$$

Eq. (106) then reads

$$\frac{\partial N}{\partial y} = \sqrt{\frac{1}{y^{d/2}} + N^2} , \qquad (111)$$

with initial condition at $y_0 = ht_0$

$$N(y_0, z) = z , \qquad (112)$$

where y_0 is a dimensionless measure of the magnetic field. Note that N only depends on the initial bias through the initial condition. The solutions of (111) for large y, and for small y and z (with logarithms for $d = 4$), are

$$N(y,z) \simeq B\,\exp(y) \quad , \quad y \gg 1 , \qquad (113)$$

$$N(y,z) \simeq A\,y^{(4-d)/4} + \left[z - A\,y_0^{(4-d)/4}\right] \quad ,$$

$$y \ll 1 \ , \ d \neq 4 , \qquad (114)$$

where $A = 4/(4-d)$ and B is a constant. Using $\sqrt{2}M = N\,y^{d/4}$ gives the corresponding behavior of $M(t)$. Note that for a negative bias N starts negative, but since from (111) its growth is always positive, N becomes large and positive for large y ($B > 0$). This can also be seen from (105): if M starts large, there is a feedback through the time integral which boosts the effect of the h field. Therefore, contrary to the scalar case (Sec. III A) the external field will always reverse the magnetization, however large $|z|$ may be. The inversion time cannot be estimated, however, without solving the full equation (111). For example, even if we set $M(t) = 0$ in (105) we cannot estimate the continued effect of $M(t')$ from t_0 to t. But if the initial bias is very small, i.e., if $|z|$ is small, N will be small from the initial time to the inversion time. Then we can set $N = 0$ in (114), giving [cf. (79)] $t_{inv}/t_0 = \exp\left(|m_0|/|ht_0|\right)$ for $d = 4$ and

$$y_{inv}^{\frac{4-d}{4}} = y_0^{\frac{4-d}{4}} + |z|/A ,$$

$$\text{or} \quad (t_{inv}/t_0)^{\frac{4-d}{4}} = 1 + |m_0'|/|ht_0|A , \qquad (115)$$

for $d \neq 4$. The late-time exponential growth of $M(t)$, which will lead to a very rapid saturation of $\left\langle\vec{\phi}\right\rangle$, can be understood from the nonlinear equation of motion (98). Keeping the important terms at late times and writing $\vec{m} = \rho\hat{\vec{m}}$ yields $\dot{\hat{\vec{m}}} = \vec{h}_\perp$ and $\dot{\rho} = \rho\vec{h}_\parallel$. Hence $\rho \sim \exp(h_\parallel t)$. So, despite the large-$n$ treatment of $\vec{m}$ we self-consistently obtain the correct asymptotics. The scaling regime (characterized by the scale $L(t) \gg \zeta$) comprises both the "initial growth" when $M \ll 1$ [Eq. (114)] and the intermediate stage prior to saturation (when $M \gg 1$). So we want to solve (111) (numerically) to obtain the full solution for $M(t)$. The above scaling form not only simplifies the equations but also provides a more transparent picture of the combined role of the variables t, h, and m_0; namely, $1/h$ and $(ht_0)^{d/4}\sqrt{t_0}$ are the characteristic scales of time and bias.

We now consider a time-dependent external field $h(t)$. For $h(t) \geq 0$ and $h(t) = 0$ at isolated points only, we may define the following one-to-one mapping between the scaling variable and the time t:

$$y(t) = \int_0^t dt' h(t') . \qquad (116)$$

Let $t(y)$ be the inverse function of $y(t)$. By analogy with the previous case we introduce h_0, a characteristic amplitude of $h(t)$. Then, defining the scaling function

$$N(y(t),z) = \sqrt{2}M(t)/(h_0 t)^{d/4} , \qquad (117)$$

$$z = m_0'/(h_0 t_0)^{d/4} , \qquad (118)$$

and noting that $\partial N/\partial t = h(t)[\partial N/\partial y(t)]$, Eq. (106) becomes

$$\frac{\partial N}{\partial y} = \sqrt{[h_0 t(y)]^{-d/2} + N^2} , \qquad (119)$$

with initial condition (112) at $y(t) = y_0 = h_0 t_0$. The solution of (119) for y and z both small is

$$N(y,z) \simeq z + \int_{h_0 t_0}^{y(t)} dy' \left[h_0 t(y')\right]^{-d/4} \quad , \quad y \ll 1 ,$$

(120)

while the large-y solution is (113), but with y given by (116). When $h(t) = \text{const}$ this formalism reduces to the previous one. The procedure to relate the scaling variables $y_2(t)$ and $y_1(t)$ concerning two different fields $h_2(t)$ and $h_1(t)$ is to replace $h_2(t')$ by $h_2(t(y_1(t')))$ in the time integral defining $y_2(t)$. In general the function $y(t)$ will not be invertible, however, so the scaling form is of limited practical use in this case. For example, the integral

of $h(t) = h_0 \exp(-\omega t)$ is easily inverted, but the integral of $h(t) = h_0[1 - \sin(\omega t)]$ has to be inverted numerically. In practice, of course, one can always solve Eq. (106) for each given field $h(t)$. From a theoretical point of view, however, the scaling variable $y(t)$ is interesting: it shows that all that matters at a given time is the sum of the field at all previous times.

To evaluate the expectation values for the order parameter $\vec{\phi}$ in the scaling regime, we make the usual replacement $\vec{\phi}(\vec{m}) \to \hat{\vec{m}}$. Given the Gaussian initial conditions and the linearity of (102) (following from taking the large-n limit), the components of $\vec{m}(\mathbf{r}, t)$ are independent Gaussian variables with nonzero mean. Evaluating the Gaussian averages we obtain n-dependent scaling functions with arguments $M(t)$, $\gamma(1,2)$, and/or $S_0(t)$, calculated above in the large-n limit. We recall that, as far as the determination of the $\vec{m}$ moments and of the scaling functions is concerned, the leading order of the systematic approach, i.e., the large-n treatment of the $\vec{m}$ equation, is equivalent to assuming that $\vec{m}(\mathbf{r}, t)$ is a Gaussian field.

Magnetization

Evaluating the Gaussian average of the field $\vec{\phi}$, we obtain (see the Appendix)

$$\left\langle \vec{\phi}(t) \right\rangle = \left\langle \frac{\vec{m}}{|\vec{m}|} \right\rangle = \vec{M}(t) \frac{2}{\sqrt{\pi}} \int_0^1 ds\, (1-s^2)^{\frac{n-1}{2}} \exp\left[-\vec{M}^2(t) s^2\right] , \tag{121}$$

where $\vec{M}(t) = M(t)(1, 1, ...)$ follows from (100) and (101), and $M(t)$ is the solution of Eq. (106). This result reduces to the error function form (70) when $n = 1$. In the early scaling regime ($M^2 \ll 1$) we can expand the exponential in (121). Then, from (105), or using (120) and (117), we obtain

$$\begin{aligned} |\langle \vec{\phi}(t) \rangle| &\simeq \frac{B\left[1/2, (n+1)/2\right]}{\sqrt{\pi}} |\vec{M}(t)| \quad , \quad |\vec{M}(t)| \ll 1 , \\ &= \frac{B\left[1/2, (n+1)/2\right]\sqrt{n}}{\sqrt{\pi}} \left[\left(\frac{t}{t_0}\right)^{d/4} m_0' \right. \\ &\quad \left. + \int_{t_0}^{t} dt' h(t') \left(\frac{t}{t'}\right)^{d/4} \right] \end{aligned} \tag{122}$$

in close agreement with the predictions from the large-n treatment of $\vec{\phi}$ [12]. In the saturation limit ($M^2 \gg 1$) the integral in (121) is dominated by small values of s and we can expand the binomial. Using (113) and (117) for $h \neq 0$, and (105) for $h = 0$, this gives

$$|\langle \vec{\phi}(t) \rangle| = 1 - \frac{n-1}{4\vec{M}^2} + O(1/\vec{M}^4) \quad , \quad |\vec{M}(t)| \gg 1 , \tag{123}$$

$$\simeq 1 - \frac{n-1}{2n} \frac{\exp\left[-2\int_0^t dt' h(t')\right]}{(t/t_0)^{d/2}} \quad , \quad h \neq 0 , \tag{124}$$

$$\simeq 1 - \frac{n-1}{2n} \frac{1}{m_0'^2 (t/t_0)^{d/2}} \quad , \quad h = 0 . \tag{125}$$

Hence the magnetization saturates exponentially fast in the presence of an external field, and as a power law when there is only an initial bias. Again, this agrees with the large-n limit of $\vec{\phi}$ [12,19]. As expected, the magnetization induced by the external field always dominates over the initial bias at late times. In other words, the system loses the memory of its initial condition. This differs from the scalar case, where both h and m_0 contribute to the exponential behavior [cf. (73)]. The magnetization curves for the full time range are shown in Fig. 2 for different values of n and h.

Although the transverse magnetization is zero by symmetry, the coefficient $(n-1)$ in (124) suggests that the leading correction to saturation is due to the part of $\vec{\phi}$ transverse to $\vec{h}$. This is easy to understand: recall that $\vec{\phi}$ quickly saturates in length in any direction, hence the time increase in the net component of $\vec{\phi}$ along $\vec{h}$ must come from rotation.

Pair correlations

The Gaussian calculation of the two-time pair correlation function of $\vec{\phi}$ is relatively straightforward, though the algebra is rather long (see the Appendix). The simplest way we found to express the result is the following:

$$\begin{aligned} C(1,2) &= \left\langle \hat{\vec{m}}(1) \cdot \hat{\vec{m}}(2) \right\rangle \\ &= \frac{4}{\pi} \int_0^1 du \int_0^1 dv \left[\frac{n}{2}\gamma + \vec{M}(1)\cdot\vec{M}(2) - \frac{\alpha(u,v)}{\beta(u,v)}\gamma \right] \\ &\quad \times \frac{\left[(1-u^2)(1-v^2)\right]^{\frac{n-1}{2}}}{\beta(u,v)^{\frac{n+2}{2}}} \exp\left\{ -\frac{\alpha(u,v)}{\beta(u,v)} \right\} , \end{aligned} \tag{126}$$

$$\begin{aligned} \alpha(u,v) &= \vec{M}^2(1)u^2 + \vec{M}^2(2)v^2 \\ &\quad -2\gamma(1,2)\vec{M}(1)\cdot\vec{M}(2)u^2v^2 , \\ \beta(u,v) &= 1 - \gamma^2(1,2)\, u^2 v^2 . \end{aligned} \tag{127}$$

$\vec{M}(i)$ is the same as in (121), and $\gamma(1,2)$ is given by (68). The equal-time correlation function $C(x, M)$ is shown in Fig. 3 for different values of n and constant field h (the same values as in Fig. 2).

An especially convenient algorithm for numerical integration is obtained with the substitutions $u = \cos(a)$ and $v = \cos(b)$: this yields a factor $[\sin(a)\sin(b)]^n$ in the integrand making its singularity for $\gamma = 1$ (equal times) explicitly integrable. The scaling function (126) generalizes the usual BPT scaling function to an off-critical system, and indeed it reduces to (43) when $M = 0$. It can be checked that any choice of axis, different from (100), produces the same result (126). The transverse and longitudinal parts of $C(1,2)$ (relative to $\vec{h}$) can be read off from the big square bracket in the integrand: the transverse contribution arises from the term $(n-1)\gamma/2$, while the longitudinal one arises from $(1/2 - \alpha/\beta)\gamma + \vec{M}(1)\cdot\vec{M}(2)$.

When $n = 1$ (126) should reduce to (80) [with $\langle\phi\rangle$ given by (70)]. To show this one must express (126) as a single integral using appropriate variable changes. Although we have not been able to give an analytical proof, we have verified the equivalence to great numerical accuracy. Another check on (126) is the large-n limit, which gives $\langle\vec{m}(1)\cdot\vec{m}(2)\rangle / [\langle\vec{m}^2(1)\rangle\langle\vec{m}^2(2)\rangle]^{1/2}$, as expected.

When $\gamma \to 0$ with fixed $M(1)$ and $M(2)$, i.e., $r \to \infty$ with fixed times, the correlations decay as [compare (85) for $n = 1$]

$$C(1,2) = \left\langle\vec{\phi}(1)\right\rangle\cdot\left\langle\vec{\phi}(2)\right\rangle + a(t_1,t_2)\,\gamma + O(\gamma^2)\ , \qquad (128)$$

where $a(t_1,t_2)$ is a known function of $\vec{M}(1)$ and $\vec{M}(2)$. It also interesting to look at the decay of the autocorrelation function $A(t_1,t_2) = C(0,t_1,t_2)$ when $t_2 \gg t_1 = t_0$, $h = 0$, and $m_0 \neq 0$. In this case (105) and (68) give $M(1) \sim m_0'$, $M(2) \sim M(1)/\gamma$, and $\gamma \sim (t_1/t_2)^{d/4}$. A careful expansion of (126) then yields

$$A(t_1,t_2) = |\langle\vec{\phi}(t_1)\rangle|\left[1 + \frac{(n-1)B}{m_0^2}\left(\frac{t_1}{t_2}\right)^{d/2} + O(\gamma^4)\right],$$

$$t_2 \gg t_1\ , \qquad (129)$$

where $B = (2^{(d+2)/2} - 1)/2$. As expected, the saturation limit of the autocorrelations is the initial bias in the field $\vec{\phi}$. The coefficient $(n-1)$ indicates a contribution from rotation, as in (124).

Density of defects

Finally, we evaluate the average density of defect core volume per unit volume of the system, $\rho_{def}(t)$. The Gaussian calculation follows the same steps as in the previous section for a scalar system. This gives

$$\rho_{def}(t) = \langle\delta(\vec{m})\rangle = [P(0)]^n = \left(\frac{d}{8\pi}\right)^{n/2}\frac{\exp\left[-\vec{M}^2(t)\right]}{t^{n/2}}\ , \qquad (130)$$

which generalizes (88). $P(m)$ is the one-point distribution for each component of $\vec{m}$, given by (87). For $m_0 = h = 0$ (130) gives the usual scaling form $\rho_{def} \sim L^{d-n}/L^d \sim 1/L^n$.

C. Comparison with experiment: Two-dimensional XY model with bias

For systems with $d = n = 2$ the defects are vortices and antivortices interacting strongly below the transition temperature (known as the "Kosterlitz-Thouless" transition temperature; see, e.g., [20]). The energy of a vortex pair is of order $\ln(L/\zeta)$, with ζ the vortex core size and L the vortex pair separation. If scaling holds, then the defect density $\rho_{def}(t)$ should scale as $L^{-2}(t)$ [Eq. (130)]. The product of these two results then gives the energy density, $\epsilon \sim \ln(L/\zeta)/L^2$.

The planar XY model is of particular interest since it appears to be a special case: there are no conclusive predictions or definitive measurements regarding the asymptotic growth in this system, but there are indications that the growth is anomalous. Yurke *et al.* [21] have suggested a slower growth law $L \sim (t/\ln t)^{1/2}$ for nonconserved systems, and indeed it has proven difficult to reach the scaling regime through numerical simulations (see, e.g., [8, 21] and references therein). More recently, Bray and Rutenberg [22] concluded that the energy dissipation due to the ordering process occurs significantly on all scales between ζ and the intervortex spacing $L(t)$, suggesting that there may not be a single characteristic length scale in the system, i.e., that the scaling hypothesis may not hold in this case. On the assumption that scaling *does* hold, however, the $(t/\ln t)^{1/2}$ growth is recovered [25]. Numerical simulations [23] also provide evidence that the scale $L(t)$ required to collapse the data for the pair correlation function, and the typical intervortex spacing $\rho(t)^{-1/2}$, are not simply proportional to each other.

The systematic approach cannot account for these possible logarithmic effects since, as a consequence of treating the dynamics of the field $\vec{m}$ in the large-n limit, a $t^{1/2}$ growth is predicted for all n and d. For the same reason, it also gives the incorrect value $d/2$ for the exponent λ [Eq. (78)]. It is still interesting, however, to make a qualitative comparison between the theory and experimental or simulation data; namely, to confront the effect of the initial bias in the results.

Pargellis, Green, and Yurke (PGY) [8] have devised an experimental system exhibiting planar XY-model behavior. The system consists of a nematic liquid crystal material placed between two plates. A suitable choice of the temperatures at the two plates creates a nematic-isotropic interface (parallel to the plates) near the center of the cell, where the nematic director has a fixed angle with the normal axis. Hence the projection of the director onto the interface provides the xy degree of freedom. In addition, a normal alignment is imposed at the colder plate, creating a splay of the director from this plate to the interface. With these boundary conditions the symmetry $\vec{\phi} \to -\vec{\phi}$ is effectively broken (i.e., there are no defects with charge 1/2) and at the interface the defects look like vortices. After inducing a thermal quench in this system, PGY measured the density of defects $\rho(t) = \rho_{def}(t)$, the autocorrelation function $A(t,t_0)$, and the magnetization $\left\langle\vec{\phi}(t)\right\rangle$. To confirm that the system is governed by the XY-model dynamics, PGY performed numerical simulations of this model using as initial condition not a random field configuration, but rather one obtained from experiment. Although they found good agreement between the results, these did not exhibit the expected scaling behavior $\rho(t) \sim t^{-1}$ and $A(t,t_0) \sim t^{-(d-\lambda)/2} \sim t^{-0.585}$ (where the latter follows from Mazenko's theory [6, 24]), indicating that some aspect of the initial condition was preventing the system from reaching the scaling regime. To study the effect of a nonuniform distribution for the angle θ between the initial field $\vec{\phi}(t_0)$ and the x axis, PGY performed simulations using the probability distribution

$$P(\theta) = \frac{1}{2\pi}\left[1 + A\cos(k\theta)\right]\ , \qquad (131)$$

where A is the "bias parameter," and $k = 1$ corresponds to a dipolar deviation from uniformity. Higher order distortions ($k \geq 2$) were shown to produce a late-time behavior indistinguishable from the one with zero bias ($A = 0$), and therefore were excluded. The log-log plots of the simulation data (with different values of A) for $\rho(t)$, $A(t,t_0)$, and $|\langle\vec{\phi}(t)\rangle|/|\left\langle\vec{\phi}(t_0)\right\rangle|$ are shown in Figs. 4, 6, and 8 below. The corresponding log-log plots from the systematic approach (Sec. III B), obtained using the relation $M(t_0) = A/\sqrt{2\pi}$ (see below), are shown in Figs. 5, 7, and 9 below. Taking into account that the scales of time are arbitrary, there appears to be a good qualitative agreement between the theory and the simulations, namely, in the manner in which the curves change with the bias parameter A. PGY found that the best fit of the simulations to the experimental data is for $A = 0.07$. At late times, the simulation data and the theoretical curves for $\rho(t)$ (Figs. 4 and 5) drop below the line t^{-1} (the expected decay for $A = 0$), as a consequence of the initial bias. This is what we expect from (130) and (105), which give $\rho(t) \sim \exp(-t\,m_0^2)/t$. From the zero-bias autocorrelations (expected to decay as $t^{-(d-\lambda)/2}$) PGY measured $(d-\lambda)/2 = 0.543 \pm 0.009$, while the corresponding results from Mazenko's theory and from the systematic approach are $(d-\lambda)/2 = 0.585$ (solid line in Fig. 6) and $(d-\lambda)/2 = 0.5$ (solid line in Fig. 7). For $A \neq 0$, the autocorrelation curves do not decay indefinitely, but have a saturation limit which is the initial bias $\phi_0 = |\langle\vec{\phi}(t_0)\rangle|$. This is what we expect from (129) which gives $\ln[A(t,t_0)] \simeq \ln(\phi_0) + 1/(m_0^2 t)^{d/2}$ for $t \gg t_0$. The solid lines in Figs. 8 and 9, with slopes $\lambda = 0.83$ and $\lambda = 1$, describe the initial growth of the magnetization [cf. (122)]. The fits to the simulation data ($A = 0.07$) and to the experimental data, however, give $\lambda = 0.518 \pm 0.021$. The magnetization curves with the larger values of A indicate that the system is close to saturation, and therefore outside the scaling regime. This behavior is described by (125). Since the experimental and simulation results do not respect the usual scaling forms in part because of the bias, they are inconclusive about the existence of logarithmic factors in $L(t)$.

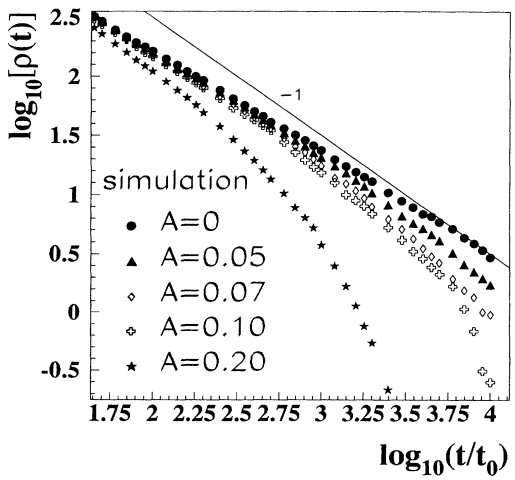

FIG. 4. Density of defects for the 2D XY model. Simulation data from Pargellis *et al.* [8]. There is no applied field and A is the bias parameter [Eq. (131)]. The solid line with slope -1 is the expected asymptotic behavior.

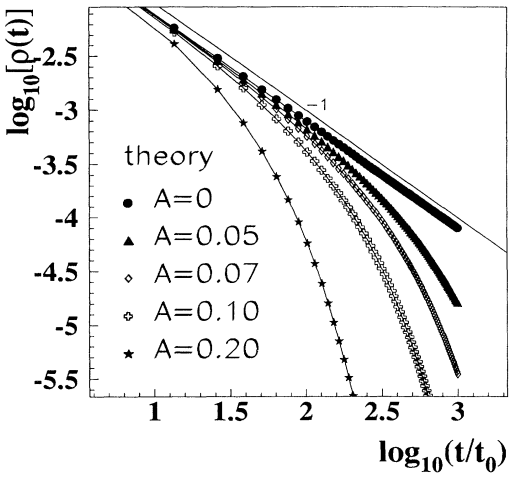

FIG. 5. Density of defects for the 2D XY model, as predicted by the systematic approach. There is no applied field, and the initial bias is given by $M(t_0) = A/(2\pi)^{1/2}$.

In order to compare the theory with the PGY data, we calculated the probability distribution of θ corresponding to a Gaussian distribution of the initial auxiliary field $\vec{m}(\mathbf{r},t_0)$. Since $P(\theta)$ in (131) is maximum for $\theta = 0$, θ is the angle between $\vec{m} = \vec{m}(t_0)$ and the most probable direction $\vec{m}_0 \equiv \langle\vec{m}(t_0)\rangle$, i.e., $\mu = \cos(\theta) = \vec{\phi}(t_0)\cdot\left\langle\vec{\phi}(t_0)\right\rangle = \hat{\vec{m}}\cdot\hat{\vec{m}}_0$. Noting that $P(\vec{m})$ is the product of two distributions of the form (87), using polar coordinates, exploiting the symmetry of $\cos(\theta)$, and making the substitution $s = \cos(\theta)$, we obtain

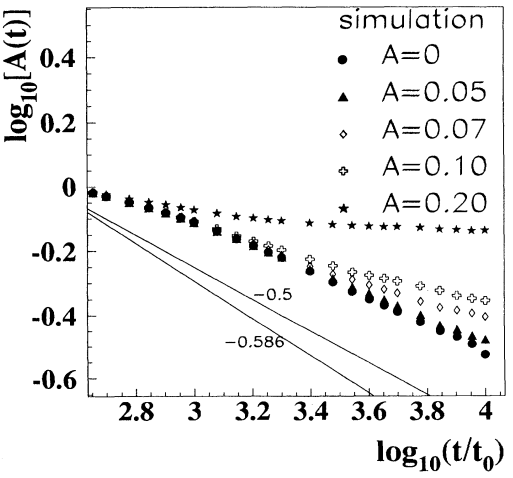

FIG. 6. Autocorrelation function for the 2D XY model. Simulation data from Pargellis *et al.* [8]. The solid lines with slopes -0.5 and -0.586 are the asymptotic decays predicted by the systematic approach and by Mazenko's approach [5, 6].

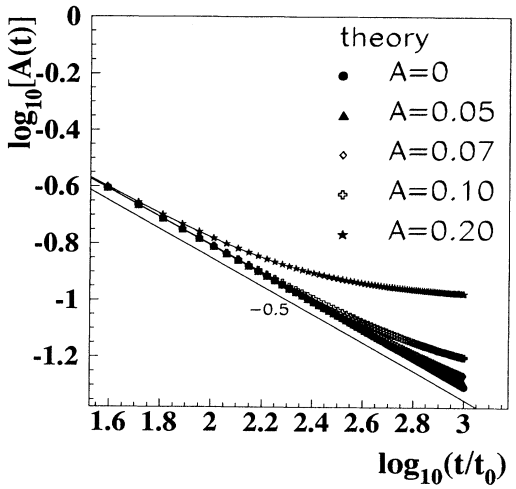

FIG. 7. Autocorrelation function for the 2D XY model, as predicted by the systematic approach.

$$P(\mu) = \int d\vec{m}\, P(\vec{m})\delta(\mu - \hat{\vec{m}}\cdot\hat{\vec{m}}_0)$$
$$= \int_0^\infty \frac{dm\, m}{2\pi S_0} \exp\left(-\frac{m^2+m_0^2}{2S_0}\right)$$
$$\times 2\int_{-1}^{1} \frac{ds}{\sqrt{1-s^2}} \exp\left(\frac{m\, m_0\, s}{S_0}\right) \delta(\mu - s)\ .$$

Performing the integrals and noting that $P(\theta) = P(\mu)|\sin(\theta)|/2$ gives

$$P(\theta) = \frac{\exp\left(-M_0^2\right)}{2\pi}(1 + M_0\sqrt{\pi}\cos(\theta)\exp[M_0^2\cos^2(2\theta)]$$
$$\times\{1 + \mathrm{erf}[M_0\cos(\theta)]\})\ , \qquad (132)$$

where $M_0 = |\vec{M}_0| = m_0/\sqrt{2S_0}$ and $m_0 = |\vec{m}_0|$ is the initial bias. Expanding (132) when M_0 is small yields, to leading order,

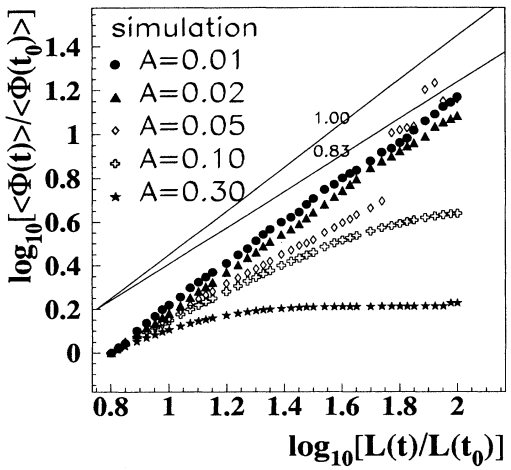

FIG. 8. Magnetization for the 2D XY model. Simulation data from Pargellis *et al.* [8]. The solid lines with slopes 1 and 0.83 describe the initial growth as predicted by the systematic approach and by Mazenko's approach [5, 6].

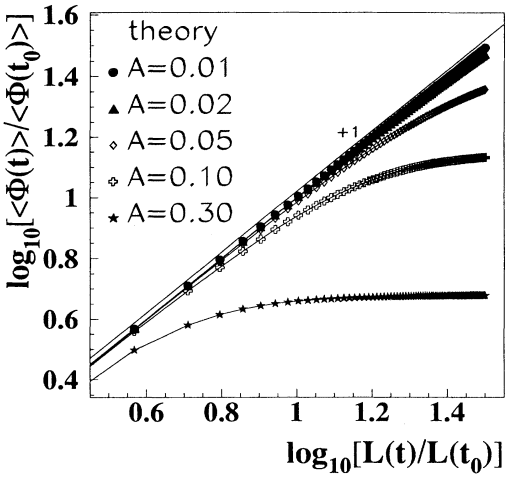

FIG. 9. Magnetization for the 2D XY model, as predicted by the systematic approach.

$$P(\theta) = \frac{1}{2\pi}\left[1 + M_0\sqrt{\pi}\cos(\theta)\right]\ . \qquad (133)$$

Comparing with (131) gives $M(t_0) = M_0/\sqrt{2} = A/\sqrt{2\pi}$, which we used to calculate the theoretical plots for given values of A.

IV. CONCLUSIONS

Off-critical quenches in phase-ordering systems with nonconserved order parameters are of experimental interest, as the conditions of perfect symmetry required for critical quenches may be difficult to ensure [8].

We have extended the "systematic approach," developed by Bray and Humayun for critical quenches [9], to investigate the asymptotic ordering dynamics of nonconserved quenched systems with an external field and an initial bias. An important difference relative to critical quenches is that as the phase symmetry is broken the system evolves more rapidly towards final equilibrium. In particular, as the topological defects disappear more rapidly the scaling regime, characterized by the length scale $L(t) \sim \sqrt{t}$, has a more limited duration.

A key ingredient of the approach is to identify the important effect of the external field in the ordering process, which is a wall driving force for scalar systems and bulk rotation for vector systems. This allowed us to make convenient choices for the potential driving forces $[V_1'(\phi;h)$ and $\vec{U}(\vec{\phi};\vec{h})]$ and to introduce a meaningful auxiliary field. Treating the auxiliary field dynamics in the large-d (or large-n) limit, we were then able to calculate the magnetization [Eqs. (70) and (121)], the pair correlation function [Eqs. (80) and (126), which extend the standard OJK and BPT scaling functions to off-critical quenches] and the density of defects [Eqs. (88) and (130)], for scalar and for vector systems.

The magnetization and the pair correlations are shown in Figs. 1–3, for particular choices of n, d, m_0, and $h(t)$. These results have been studied in various limiting cases: Eqs. (73) and (74) for $\langle\phi\rangle$, Eqs. (122)–(125) for $\langle\vec{\phi}\rangle$, Eqs. (84) and (85) for $C(1,2)$ with $n = 1$, and Eqs. (128)

and (129) for $C(1,2)$ with $n > 1$. The respective behaviors have been discussed and are well understood and in accord with our expectations. We find, in particular, that the saturation of the magnetization and the decay of the defect density are exponentially fast. The initial growth of the magnetization [Eqs. (73)–(122)] agrees well with previous predictions by BK [12] based both on the large-n solution for $\vec{\phi}$ and on general scaling arguments. We also compared our results for a biased two-dimensional (2D) XY model with numerical simulation data [8] (Sec. III C and Figs. 4–9), and found good qualitative agreement. These simulation data, on the other hand, had been found to agree well (for a certain value of the initial bias) with data from experiments on nematic liquid crystals [8].

Finally, we recall that the auxiliary field formulation relies on the existence of stable topological defects, which govern the asymptotic dynamics of the system. One legitimate question, therefore, is whether these defects will ever form in the presence of an external field, or a bias, before the system orders completely. Clearly, the defects will form, and an intermediate scaling regime will occur [where $L(t)$ is the typical interdefect distance] if the field and the initial bias are not too strong.

ACKNOWLEDGMENTS

We thank A. N. Pargellis *et al.* [8] for making their raw data available. We thank the Isaac Newton Institute, Cambridge (A.B. and S.P.), and the Physics Departments of the Universities of Illinois and Manchester (S.P.) for hospitality. J.F. thanks JNICT (Portugal) for support.

APPENDIX: GAUSSIAN EXPECTATION VALUES

In this Appendix we indicate how to perform the calculation of the Gaussian expectation values which were stated throughout this paper. The standard results for $h = m_0 = 0$ can be obtained as particular cases of the off-critical results.

For a scalar field, $\phi = \mathrm{sgn}(m)$, m is a Gaussian variable with nonzero mean, correlator $\gamma = \langle m(1)m(2)\rangle_c / [S_0(1)S_0(2)]^{1/2}$ and second moment $S_0 = \langle m^2 \rangle_c$ [Eq. (67)]. We recall that $M = \langle m \rangle / \sqrt{2S_0}$ [Eq. (71)]. For vector fields, $\vec{\phi} = \vec{m}/|\vec{m}|$, we conveniently set the external field $\vec{h}$ and the initial bias $\vec{m}_0$ in the direction $(1,1,...)$ [Eqs. (100) and (101)]. Hence the components of $\vec{m}$, generally represented by m, are independent Gaussian variables with the same moments as above. We recall that $\vec{M} = \langle \vec{m} \rangle / \sqrt{2S_0} = \langle m \rangle (1,1,...)$. We will need the following integral representations:

$$\mathrm{sgn}(m) = \frac{1}{i\pi} \int_{-\infty}^{\infty} \frac{dz}{z} \exp\left(\frac{izm}{\sqrt{2S_0}}\right) , \tag{A1}$$

$$\frac{1}{|\vec{m}|} = \frac{1}{\sqrt{2\pi S_0}} \int_0^{\infty} \frac{dz}{\sqrt{z}} \exp\left(-\frac{z\vec{m}^2}{2S_0}\right) . \tag{A2}$$

1. Magnetization

Using the one-point Gaussian distribution (87), it is easy to obtain the following results:

$$\left\langle \exp\left(\frac{izm}{\sqrt{2S_0}}\right) \right\rangle = \exp\left(izM - \frac{z^2}{4}\right) , \tag{A3}$$

$$\left\langle \exp\left(-\frac{zm^2}{2S_0}\right) \right\rangle = \frac{1}{\sqrt{z+1}} \exp\left(-\frac{zM^2}{z+1}\right) , \tag{A4}$$

$$\left\langle \frac{m}{\sqrt{2S_0}} \exp\left(-\frac{zm^2}{2S_0}\right) \right\rangle = \frac{M}{z+1} \left\langle \exp\left(-\frac{zm^2}{2S_0}\right) \right\rangle . \tag{A5}$$

First we consider a scalar field ϕ. Using the representation (A1) and the result (A3), we can write the average value of ϕ as

$$\langle \phi \rangle = \langle \mathrm{sgn}(m) \rangle = \frac{1}{i\pi} \int_{-\infty}^{\infty} \frac{dz}{z} \exp\left(izM - \frac{z^2}{4}\right) . \tag{A6}$$

Differentiating with respect to M, completing the squares, and performing the integral gives $d\langle \phi \rangle / dM = (2/\sqrt{\pi}) \exp(-M^2)$. Finally, integrating with respect to M, with boundary condition $\langle \phi(M=0) \rangle = 0$, gives

$$\langle \phi \rangle = \frac{2}{\sqrt{\pi}} \int_0^M dx \exp(-x^2) = \mathrm{erf}(M) , \tag{A7}$$

which is the same as (72).

Now we consider a vector field $\vec{\phi}$. Using the representation (A2) and the results (A4) and (A5), and exploiting the rotational symmetry in the $\vec{m}$ space, we can write the average value of $\vec{\phi}$ as

$$\left\langle \vec{\phi} \right\rangle = \left\langle \frac{\vec{m}}{|\vec{m}|} \right\rangle = \frac{(1,1,...)}{\sqrt{\pi}} \int_0^{\infty} \frac{dz}{\sqrt{z}} \left\langle \frac{m}{\sqrt{2S_0}} \exp\left(-\frac{zm^2}{2S_0}\right) \right\rangle \left\langle \exp\left(-\frac{zm^2}{2S_0}\right) \right\rangle^{n-1}$$
$$= \frac{\vec{M}}{\sqrt{\pi}} \int_0^{\infty} \frac{dz}{\sqrt{z}(z+1)^{\frac{n+2}{2}}} \exp\left(-\frac{zM^2}{z+1} n\right) .$$

Using the substitution $s = \sqrt{z/(z+1)}$, we then obtain

$$\left\langle \vec{\phi} \right\rangle = \vec{M} \frac{2}{\sqrt{\pi}} \int_0^1 (1-s^2)^{\frac{n-1}{2}} \exp\left(-s^2 M^2 n\right) , \tag{A8}$$

which is the same as (121), and clearly reduces to (A7) when $n = 1$.

Pair correlations

Using the Gaussian joint distribution for the variables $m(1)$ and $m(2)$ [which may be the same components of $\vec{m}(1)$ and $\vec{m}(2)$], one can prove the following results, with the notation $m_1 = m(1)$, $S_1 = S_0(1)$, $M_1 = M(1)$, and $\delta = 1 - \gamma^2$:

$$\left\langle \exp\left(\frac{iz_1 m_1}{\sqrt{2S_1}} + \frac{iz_2 m_2}{\sqrt{2S_2}}\right)\right\rangle = \exp\left(iz_1 M_1 + iz_2 M_2 - \frac{z_1^2 + z_2^2 + 2z_1 z_2 \gamma}{4}\right) \tag{A9}$$

$$\left\langle \exp\left(-\frac{z_1 m_1^2}{2S_1\delta} - \frac{z_2 m_2^2}{2S_2\delta}\right)\right\rangle = \left(\frac{1-\gamma^2}{B_{12}}\right)^{1/2} \exp\left(-\frac{A_{12}}{B_{12}}\right) , \tag{A10}$$

$$\left\langle \frac{m_1 m_2}{2\delta\sqrt{S_1 S_2}} \exp\left(-\frac{z_1 m_1^2}{2S_1\delta} - \frac{z_2 m_2^2}{2S_2\delta}\right)\right\rangle = \frac{1}{B_{12}}\left[\frac{\gamma}{2} + M_1 M_2 - \gamma\frac{A_{12}}{B_{12}}\right] \times \left\langle \exp\left(-\frac{z_1 m_1^2}{2S_1\delta} - \frac{z_2 m_2^2}{2S_2\delta}\right)\right\rangle , \tag{A11}$$

with the definitions

$$A_{12} = M_1^2 z_1 + M_2^2 z_2 + \Gamma(\gamma) z_1 z_2 ,$$
$$B_{12} = (z_1+1)(z_2+1) - \gamma^2 ,$$

where $\Gamma(\gamma)$ is given by (81).

First we consider a scalar field ϕ. Using the representation (A1) and the result (A9), we can write the correlation function of ϕ as

$$C(1,2) = \langle \mathrm{sgn}(m_1)\mathrm{sgn}(m_2)\rangle = -\frac{1}{\pi^2}\int_{-\infty}^{\infty} \frac{dz_1 dz_2}{z_1 z_2} \exp\left(iz_1 M_1 + iz_2 M_2 - \frac{z_1^2 + z_2^2 + 2z_1 z_2\gamma}{4}\right) .$$

Differentiating with respect to γ, completing the squares, and performing the integrals gives $\partial C(1,2)/\partial\gamma = (2/\pi)\exp[-\Gamma(\gamma)]/\sqrt{1-\gamma^2}$. Finally, integrating with respect to γ, with boundary condition $C(\gamma = 0) = \langle\phi(1)\rangle\langle\phi(2)\rangle$, gives

$$C(1,2) = \frac{2}{\pi}\int_0^{\gamma} \frac{dy}{\sqrt{1-y^2}} \exp[-\Gamma(y)] + \langle\phi(1)\rangle\langle\phi(2)\rangle , \tag{A12}$$

which is the same as (80). For critical quenches, $\Gamma = \langle\phi\rangle = 0$, and (A12) reduces to the OJK scaling function $(2/\pi)\sin^{-1}\gamma$.

Now we consider a vector field $\vec{\phi}$. Using the representation (A2) [with the substitution $z \to z/(1-\gamma^2)$] and the results (A10) and (A11), and exploiting the rotational symmetry in the $\vec{m}$ space, we can write the correlation function of $\vec{\phi}$ as

$$C(1,2) = \left\langle \frac{\vec{m}_1}{|\vec{m}_1|}\cdot\frac{\vec{m}_2}{|\vec{m}_2|}\right\rangle = \frac{n}{\pi}\int_0^{\infty}\frac{dz_1 dz_2}{\sqrt{z_1 z_2}} \left\langle \frac{m_1 m_2}{2\delta\sqrt{S_1 S_2}} \exp\left(-\frac{z_1 m_1^2}{2S_1\delta} - \frac{z_2 m_2^2}{2S_2\delta}\right)\right\rangle \left\langle \exp\left(-\frac{z_1 m_1^2}{2S_1\delta} - \frac{z_2 m_2^2}{2S_2\delta}\right)\right\rangle^{n-1}$$
$$= \frac{1}{\pi\delta}\int_0^{\infty}\frac{dz_1 dz_2}{\sqrt{z_1 z_2}} \left[\frac{n\gamma}{2} + \vec{M}_1\cdot\vec{M}_2 - n\gamma\frac{A_{12}}{B_{12}}\right] \left(\frac{1-\gamma^2}{B_{12}}\right)^{\frac{n+2}{2}} \exp\left(-n\frac{A_{12}}{B_{12}}\right) .$$

Using the substitutions $u = z_1/(z_1 + 1 - \gamma^2)$ and $u = z_2/(z_2 + 1 - \gamma^2)$ then gives

$$C(1,2) = \frac{4}{\pi}\int_0^1 du dv \left[\frac{n}{2}\gamma + \vec{M}_1\cdot\vec{M}_2 - \gamma\frac{\alpha_{12}}{\beta_{12}}\right] \frac{\left[(1-u^2)(1-v^2)\right]^{\frac{n-1}{2}}}{\beta_{12}^{\frac{n+2}{2}}} \exp\left\{-\frac{\alpha_{12}}{\beta_{12}}\right\} , \tag{A13}$$

which is the same as (126), with α_{12} and β_{12} given by (127). For critical quenches, $\vec{M}_1 = \vec{M}_2 = \vec{0}$, and (A13) reduces to the BPT function (43).

[1] For a recent review, see A. J. Bray, Adv. Phys. **43**, 357 (1994).
[2] I. Chuang, R. Durrer, N. Turok, and B. Yurke, Science **251**, 1336 (1991); A. P. Y. Wong, P. Wiltzius, and B. Yurke, Phys. Rev. Lett. **68**, 3582 (1992); M. J. Bowick, L. Chandar, E. A. Schiff, and A. M. Srivastava, Science **263**, 943 (1994).
[3] T. Ohta, D. Jasnow, and K. Kawasaki, Phys. Rev. Lett. **49**, 1223 (1982).
[4] K. Kawasaki, M. C. Yalabik, and J. D. Gunton, Phys. Rev. A **17**, 445 (1978).
[5] F. Liu and G. F. Mazenko, Phys. Rev. B **45**, 6989 (1992).
[6] A. J. Bray and K. Humayun, J. Phys. A **25**, 2191 (1992).
[7] A. J. Bray and S. Puri, Phys. Rev. Lett. **67**, 2670 (1991); H. Toyoki, Phys. Rev. B **45**, 1965 (1992).
[8] A. N. Pargellis, S. Green, and B. Yurke, Phys. Rev. E **49**, 4250 (1994).
[9] A. J. Bray and K. Humayun, Phys. Rev. E **48**, 1609 (1993).
[10] S. De Siena and M. Zannetti [Phys. Rev. E **50**, 2621 (1994)] have developed an alternative systematically improvable approximation scheme.
[11] J. G. Kissner and A. J. Bray, J. Phys. A **26**, 1571 (1993).
[12] A. J. Bray and J. G. Kissner, J. Phys. A **25**, 31 (1992).
[13] S. M. Allen and J. W. Cahn, Acta Metall. **27**, 1085 (1979).
[14] G. F. Mazenko, Phys. Rev. Lett. **63**, 1605 (1989); Phys. Rev. B **42**, 4487 (1990).
[15] Y. Oono and S. Puri, Mod. Phys. Lett. **2**, 861 (1988).
[16] For example, for a spherical domain with $\phi = \mathrm{sgn}(h)$ and radius R these forces (in the direction of the center) are $\Delta V/\Delta\phi \sim -h$ and $(d-1)\Sigma/R$, respectively.
[17] A. J. Bray, Phys. Rev. E **47**, 228 (1993).
[18] F. Liu and G. F. Mazenko, Phys. Rev. B **46**, 5963 (1992).
[19] F. de Pasquale, D. Feinberg, and P. Tartaglia, Phys. Rev. B **36**, 2220 (1987).
[20] N. Goldenfeld, *Lectures on Phase Transitions and Renormalization Group* (Addison-Wesley, Reading, MA, 1992).
[21] B. Yurke, A. N. Pargellis, T. Kovacs, and D. A. Huse, Phys. Rev. E **47**, 1525 (1993).
[22] A. J. Bray and A. D. Rutenberg, Phys. Rev. E **49**, R27 (1994).
[23] R. E. Blundell and A. J. Bray, Phys. Rev. E **49**, 4925 (1994).
[24] F. Liu and G. F. Mazenko, Phys. Rev. B **45**, 4656 (1992).
[25] A. D. Rutenberg and A. J. Bray, Phys. Rev. E **51**, 5499 (1995).